

IMPLEMENTATION OF 5G TECHNOLOGIES WITH
HETEROGENEOUS COOPERATIVE SPECTRUM SENSING AND LTE-R

by

Kuldeep S. Gill

A Thesis
Submitted to the Faculty
of the
WORCESTER POLYTECHNIC INSTITUTE
in partial fulfillment of the requirements for the
Degree of Master of Science
in
Electrical and Computer Engineering
by

December 2017

APPROVED:

Professor Alexander Wyglinski, Major Advisor

Professor Kaveh Pahlavan

Dr. Travis Collins

Abstract

There have been an unprecedented increase in demand for high data rates and mobility required by new wireless applications which has led to intensive research on fifth generation (5G) wireless communication system. By 2020, 5G is projected to be employed worldwide supporting the connectivity of up to 20 billion devices and will be crucial in the success of vehicular networking and internet of things (IoT). It is also believed that 5G systems would be capable of providing significant improvements in cell capacity and will support high data rates up to 5 and 50 Gb/s for high-mobility and pedestrian users, respectively. However, to achieve such data rates for high-mobility scenarios there are still many challenges for wireless system engineers.

In this thesis, we propose two test-beds namely Heterogeneous Cooperative Spectrum Sensing (CSS) and Long Term Evolution for Railways (LTE-R) performance analysis test-bed to further advance the 5G system development. Heterogeneous CSS test-bed is implemented using Software-Defined Radios (SDRs) with different radio characteristics. We used both soft and hard data fusion schemes to compare the signal source detection performance in real-time fading scenario. For 5G technologies, the most effective solution is to use the underutilized spectrum as a secondary user via dynamic spectrum access (DSA). It is very challenging to get an accurate estimate of incumbent users with a single-sensor system under a practical fading environment. Various non-idealities such as shadowing, multipath and fluctuating noise variance can make it difficult to detect the primary user. Cooperative spectrum sensing can mitigate the effects of multipath and shadowing by utilizing the spatial and temporal diversity of a multiple radio network. LTE-R test-bed analyze the performance of high speed trains (HSTs) in a tunnel environment and can be used to test 5G systems for high mobility scenario in drastically impaired channels.

Acknowledgements

I would like to express my deepest gratitude to my advisor Professor Alexander Wyglinski for his continuous guidance and support towards my course of degree. I am very thankful for the opportunity to work with him in Wireless Innovation Laboratory at Worcester Polytechnic Institute.

I want to thank Professor Kaveh Pahlavan and Dr. Travis Collins for serving on my committee and providing valuable suggestions and comments with regards to my thesis.

I would also like to thank my WILab team members Dr. Srikanth Pagadarai, Dr. Paulo Ferreira, Renato, Le and my friends Rasika, Devdip and Raunak for their immense support during my graduate studies. Finally, I'm also thankful to my parents, without their constant support I wouldn't be here.

Contents

List of Figures	5
List of Tables	7
1 Introduction	8
1.1 Motivation	8
1.2 State of the Art	10
1.3 Thesis Contributions	12
1.4 Thesis Organization	12
2 Introduction to 5G and Key Technologies	14
2.1 5G Cellular Architecture	15
2.2 Key Technologies of 5G System	18
2.2.1 Massive MIMO	19
2.2.2 Machine-to-Machine (M2M) Communication	21
2.2.3 Spectrum Regulation for 5G	24
2.3 5G using Millimeter Wave (mmWave)	26
2.4 Vehicular Communication Using 5G	28
2.5 Summary	30
3 Heterogeneous Cooperative Spectrum Sensing (CSS)	31
3.1 Cognitive Radios	31
3.2 CSS in Heterogeneous Networks	33
3.3 Software Defined Radios	35
3.3.1 Universal Software Radio Peripheral (USRP) N210 and RTL-SDR .	36
3.3.2 GNURadio and Software-Defined Radio	37
3.3.3 MATLAB	37
3.4 Summary	38
4 Long Term Evolution for Railways (LTE-R)	40
4.1 LTE-R Communication System	40
4.2 Leaky Coaxial Cable	42
4.3 Channel Impairments Inside a Tunnel	43
4.3.1 Multipath Fading	44

4.3.2 Doppler Shift	44
4.4 Two-Ray Propagation Model	45
4.4.1 Classical Two-Ray Propagation Model	45
4.4.2 Dynamic K-factor	45
4.5 Summary	45
5 Implementation	47
5.1 Overview	47
5.2 Experimental Setup for Heterogeneous CSS	47
5.2.1 Transmitter Setup for CSS Measurements	47
5.2.2 Sensor Nodes Setup	47
5.3 Hard Fusion	48
5.4 Soft Fusion	49
5.4.1 Maximum Normalized Energy Scheme	49
5.4.2 Equal Gain Combining Scheme	49
5.5 LTE-R Testbed in Matlab	49
5.5.1 HST Channel Model	50
5.5.2 LTE-R OFDMA	50
5.6 Summary	50
6 Experimental Results	55
6.1 Overview	55
6.2 Heterogeneous CSS Results	55
6.2.1 Hard Decision Combining	55
6.2.2 Soft Decision Combining	55
6.3 HST LTE-R in a Tunnel	55
6.3.1 K-factor in a Tunnel	55
6.3.2 BER Performance	55
6.3.3 Real-time BER in a Tunnel	55
6.4 Summary	55
7 Conclusions	64
7.1 Research Outcomes	64
7.2 Future Work	64
Bibliography	65
A Appendix: Heterogeneous Cooperative Spectrum Sensing Code	71
A.1 harddecisionpdproc.m	71
A.2 softharddecisionpd.m	73
A.3 spectrumsenseusrp.py	75
A.4 gnuradiotlsdrsense.py	83
B Appendix: LTE-R Analysis Code	89
B.1 kfactordist.m	89
B.2 bercalculation.m	90

List of Figures

1.1	Heterogeneous sensor network employing cooperative spectrum sensing. $RFFE_i$ and SR_i represents different front end and sampling rates for the SDR units.	9
1.2	High speed train inside a tunnel for LTE-R. D_{LOS} is the distance between transmitter and receiver, d is the distance between the LCX cable transmission slots.	11
2.1	5G Architecture	16
2.2	Massive-MIMO implementation using patch antenna arrays	19
2.3	Beamforming for $N=4, 8, 12$ and 16 linear dipole antenna elements. As the number of antenna element increases we see a sharper beam confined in a smaller region. Massive-MIMO can utilize beamforming to increase spatial gain and spectral efficiency.	21
2.4	Machine-to-Machine communication paradigm in 5G Cellular System.	22
2.5	Machine-to-Machine communication paradigm in 5G Cellular System.	25
2.6	Large-scale propagation loss for $f_c = 1$ GHz, 10 GHz, 28 Ghz and 60 GHz.	27
2.7	Vehicular communication using D2D 5G cellular communication technology.	29
3.1	The block diagram explaining the basic parts of Cognitive Radio system. The operating parameters are configured based on the characterization of the wireless environment.	32
3.2	Software defined radio pushes all the adaptive elements and data manipulation operation into software. The goal of SDR is to provide or define all of the radio operation in software.	35
3.3	GNURadio and Software-Defined Radio	38
4.1	High speed train inside a tunnel for LTE-R. D_{LOS} is the distance between transmitter and receiver, d is the distance between the LCX cable transmission slots.	41
4.2	Leaky Coaxial Cable	42
4.3	Doppler spectrum for LTE-R at different train velocities v (km/h) = 300, 400 and 500 and $f_c = 5$ GHz.	45

5.1	Experimental Test-Bed For Cooperative Sensing in Heterogeneous Network. Sensors 1, 2 and 4 are RTL-SDR units, sensor 3 is USRP N210 and TX is another USRP N210 unit which is used as a signal source for this work.	47
5.2	GNU Radio Flowgraph For Transmitter Running on USRP N210.	48
5.3	GNURadio Flowgraph For USRP and RTL-SDR sensor nodes.	48
5.4	Flowchart showing AND, OR and Majority Rule Fusion schemes..	49
5.5	Flowchart showing Equal Gain Combining Scheme.	50
5.6	Flowchart showing Maximum Normalized Energy Scheme.	51
5.7	Block diagram of a communication system through a HST channel using QPSK, 16-QAM and 64-QAM.	52
5.8	HST channel model consisting of time-series K-factor and Doppler shift caused due to velocity of the train.	53
5.9	Received LTE-R OFDM signal under HST Ricean Fading Environment. . .	54
6.1	Probability of Detection versus SNR_{avg} For Hard Decision Combining. . .	56
6.2	ROC Characteristics for Hard Decision Combining with Different SNRs. .	57
6.3	Probability of Detection versus SNR_{avg} For Soft and Hard Decision Combining.	57
6.4	K-factor versus D_{LOS} for different center frequencies $f_c = 2, 3$ and 5 GHz. .	58
6.5	Comparison of E_b/N_0 verus BER for LTE-R OFDM-QPSK modulation with different K-factors.	59
6.6	Comparison of E_b/N_0 verus BER for LTE-R OFDM-16QAM modulation with different K-factors.	60
6.7	Comparison of E_b/N_0 verus BER for LTE-R OFDM-64QAM modulation with different K-factors.	61
6.8	Comparison of E_b/N_0 verus BER for LTE-R OFDM modulation with different K-factors.	62
6.9	BER variation with time for HST with different modulation schemes of LTE-R. As the train moves towards the antenna the general trend of BER goes down with small-scale fluctuations due to varying K-factor.	63

List of Tables

2.1	Cellular Technologies Comparison between different generations of deployed digital cellular networks. Data rates, standard and implementation technology is compared for the 3G, 4G and 5G	15
5.1	Operating Characteristics of Sensor Nodes	48
5.2	Tunnel and Tx/Rx Characteristics	49

Chapter 1

Introduction

1.1 Motivation

There has been an exponential growth in the Internet landscape. The devices like smartphones, computers, laptops, tablets will continue to increase along with multitude of other devices that are connected to Internet. This has facilitated the research in dynamic spectrum access (DSA) [1, 2] for efficient utilization of spectrum resources to sustain billions of Internet of Things (IoT) devices. There has been a significant increase in the study of cognitive radios for efficiently utilizing the electromagnetic spectrum. It has been observed that the spectrum occupancy is not uniform across all frequency bands, resulting in numerous spectral white spaces [3]. To opportunistically access the idle channel, spectrum sensing is considered to be a significant technology enabling DSA. Although several spectrum sensing techniques have been proposed in the open literature, energy detection is widely used due to its low implementation complexity [4]. We discuss some of the spectrum sensing techniques along with energy detection below.

- In energy detection (ED) scheme the energy of the signal is detected in the frequency location and based on the threshold value we decide whether the signal is present or absent.
- Cyclostationary Feature Detection is a complex scheme to implement compared to ED and it is mostly used when we need to also classify the signal present based on

their modulation scheme.

- When secondary user has a priori knowledge of primary user signal, matched filter (MF) detection is applied. Detection by using matched filter needs less detection time compared to ED but primary user information is required.

These spectrum sensing techniques can be used in a non-cooperative manner but it is very challenging to get an accurate estimate using a single-sensor system under a practical fading environment. Various non-idealities such as shadowing, multipath and fluctuating noise variance can make it difficult to detect the primary user [5,6]. Cooperative spectrum sensing can mitigate the effects of multipath and shadowing by utilizing the spatial and temporal diversity of a multiple radio network [7,8]. In cooperative spectrum sensing, each sensor node collects the spectral data and transmits it to a fusion center (FC) for decision making. Figure ?? shows how a heterogeneous sensor network exploits the spatial diversity.

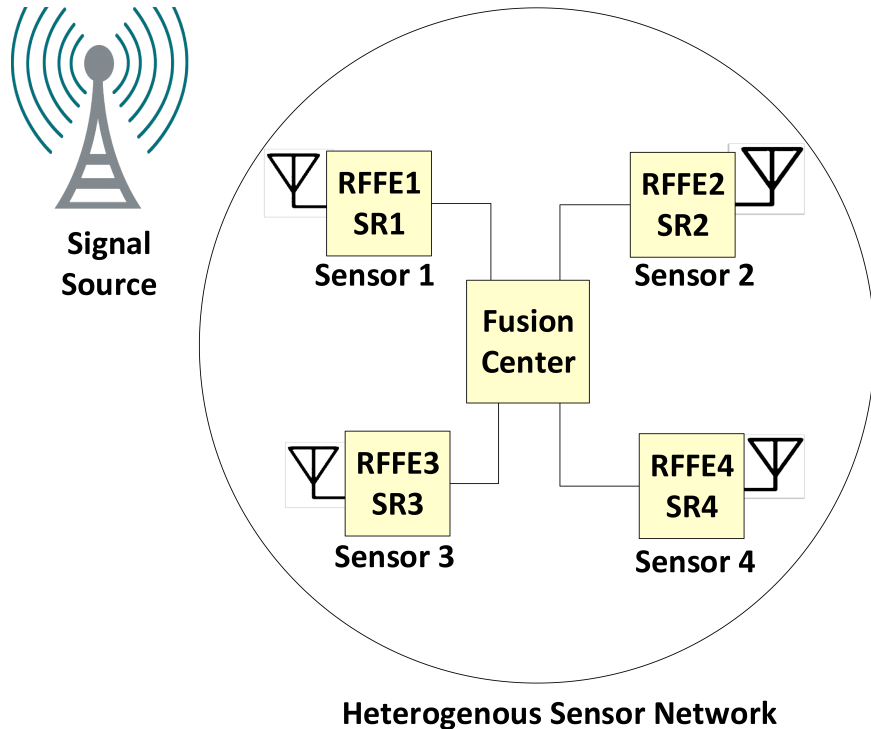


Figure 1.1: Heterogeneous sensor network employing cooperative spectrum sensing. $RFFE_i$ and SR_i represents different front end and sampling rates for the SDR units.

We have also analyze the performance of Long Term Evolution for Railways (LTE-R) in a tunnel environment. In recent years, the use of trains have witnessed tremendous growth due to their increasing speeds, which has led to the demand for reliable wireless communication systems with these transportation systems. The development of a reliable wireless network for high speed trains is not a simple task and it is still an emerging technology. Global System for Mobile Communication (GSM-R) [9], was a wireless communications standard designed for high speed trains, but it turned out not to be reliable enough and possess several limitations. Subsequently, LTE [10] proposed a promising solution for achieving broadband data rates in high speed trains that can overcome various GSM-R limitations [11, 12].

LTE-R is a high speed communication standard based on the existing LTE system architecture [12]. There has been several studies regarding the assessment of LTE-R as a viable choice for next generation high speed communications for railway applications [13, 14]. Most LTE systems operate at 1.8 GHz – 2.6 GHz bands, which possesses a high propagation loss and severe fading effects. Highly mobile trains inside tunnel environment makes the design of reliable communication links very challenging. To achieve reliable radio coverage inside tunnels, leaky feeder cables have been proposed [15]. With LCX, more uniform coverage can be achieved and installation is also comparatively simple. Each slot in the cable is equivalent to an antenna, which can transmit and receive signals. Figure ?? shows the LOS propagation environment inside a tunnel for a high speed train with velocity v .

1.2 State of the Art

The cooperative spectrum sensing testbed using normalized energy detection has been implemented and has been compared for both soft and hard data fusion scheme. Both soft data fusion and hard data fusion have been extensively studied [16–18], with several algorithms being implemented for each scheme. In a hard decision approach, each local decision statistic from sensor node is transmitted to an FC via overhead channels. The FC merges the sensing data and makes a global decision based on various algorithms such as majority rule, OR rule and AND rule [19]. For a soft decision scheme, each SU sends its local sensing data to the FC, which makes decision based on a global test statistic G . Soft

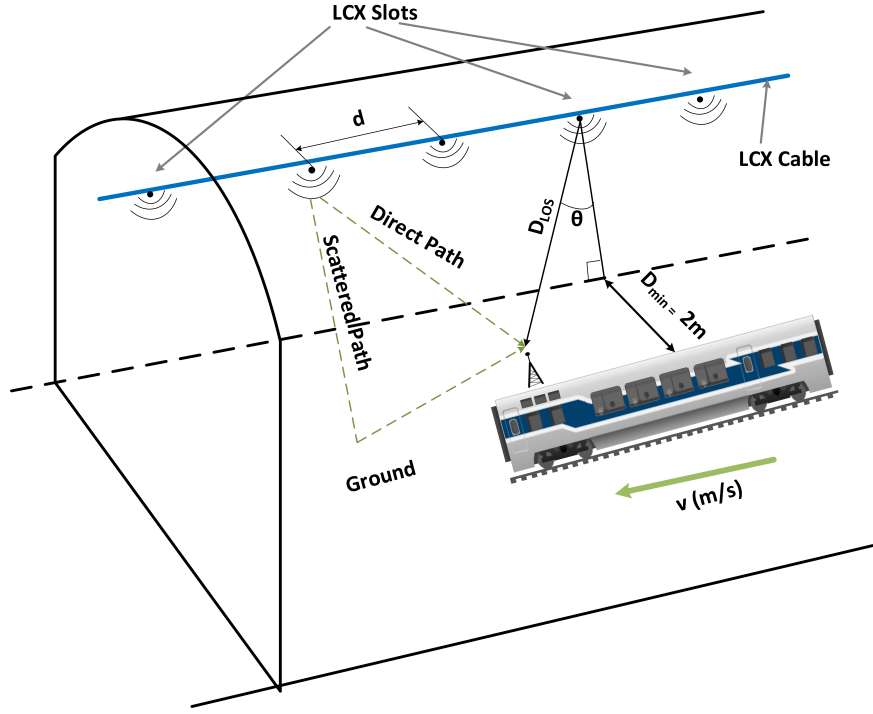


Figure 1.2: High speed train inside a tunnel for LTE-R. D_{LOS} is the distance between transmitter and receiver, d is the distance between the LCX cable transmission slots.

decision combining improves the cooperative gain but it also possesses several limitations. With an infinite bandwidth, the real floating values can be transmitted to the FC, which can lead to a reliable decision mechanism. However, due to bandwidth constraint we have to quantize the data and this leads to error in the energy values. In hard decision combining, we can just transmit the decisions of the sensor nodes to the FC which can be binary values with 1 indicating that signal source is present and 0 indicating that a signal source is absent.

In open literature, most channel modeling have considered open areas with high speed trains [13, 14], while relatively little research has been conducted in tunnel environments. Due to various challenges presented by tunnel environments, it is important to derive a channel model for LTE-R involving high speed trains. In this paper, we analyze the effects of high Doppler shift and multipath due to tunnel environments. Experimental studies conducted inside tunnel environments have shown that the field amplitude distribution fits smoothly over a Rician distribution [20]. Several research efforts have been conducted

on large-scale and small-scale fading of wideband communication systems inside tunnel environments. To the best of the authors knowledge, none of these studies have been conducted for LTE-R, which employs Orthogonal Frequency Division Multiplexing (OFDM) signals for data transmission inside tunnels. The large Doppler shifts caused by high speed trains will potentially lead to ambiguity in extracting the carrier frequency, which can drastically increase the BER [21]. Therefore, it is important to study the effects of high Doppler shift and multipath fading for LTE-R communications in tunnel environments such that equalizers can be design efficiently.

1.3 Thesis Contributions

This thesis will contribute the following to the cognitive radio communications and cellular wireless field:

- A cooperative spectrum sensing test-bed with normalized energy detection using both soft data fusion and hard data fusion implemented on available software defined radios.
- For soft data fusion, Maximum Normalized Energy (MNE) and Equal Gain Combination (EGC) algorithms are used. Hard data fusion is also implemented using majority rule, AND, and OR approaches. Both USRP N210s [22] and RTL-SDRs [23] are employed for the implementation of the heterogeneous sensor network.
- A performance assessment and simulation of LTE-R communications in a tunnel environment experiencing severe fading.
- Dynamic K-factor for a tunnel environment is derived using the classical two-ray propagation model [24] and is used to build Rician fading model for the tunnel.

1.4 Thesis Organization

This thesis will be organized into the following chapters: Chapter 2 provides background knowledge on heterogeneous cooperative spectrum sensing and focuses on heterogeneous networks, cooperative spectrum sensing and software-defined radios. Chapter 3 discusses

LTE-R in detail and provides the necessary understanding of the LTE-R implementation in a tunnel environment. Leaky Coaxial Cable (LCX) , channel impairments and two-ray propagation model is also discussed in detail. In chapter 4 and 5 implementation of heterogeneous cooperative spectrum sensing (CSS) test-bed and LTE-R performance analysis in a tunnel is discussed. Chapter 6 presents the results of the implementation of heterogeneous CSS test-bed and LTE-R in a tunnel. Chapter 7 concludes this thesis, summarizing the accomplishments and outlines possible future work.

Chapter 2

Introduction to 5G and Key Technologies

The rapid advancement in the wireless communications shows the huge success in the wireless communication system. The advancement started with second generation (2G) system's debut in 1991 which were commercially launched on the GSM standard in Finland by Radiolinja. 2G systems were significantly more spectrally efficient compared to their predecessors and 2G also introduced the data services for mobile starting with SMS text messages, picture messages and multimedia messages (MMS). From 2G we migrated to 3G system which were first launched in 2001 and had fast mobile Internet access. 3G also introduced video calls and mobile TV and was able to provide information transfer speed of at least 2 Mbit/s. The 4G wireless systems were designed to be fully based on IP telephony where all the voice communications and multimedia sessions are delivered over Internet protocol (IP) networks [25]. 4G systems use orthogonal frequency division multiplexing (OFDM), multiple-input multiple-output (MIMO), and link adaptation technologies for a long term evolution (LTE) radio interface. 4G wireless networks can support data rates of up to 1 Gb/s for low mobility and up to 100 Mb/s for high mobility scenarios. The next evolution in wireless mobile communications is the fifth generation (5G) which is expected to be deployed by 2020.

Due to a sharp increase in number of wireless mobile devices and the shortage of the

wireless spectrum, researchers have started to investigate 5G wireless technologies. It is expected that the 5G network will achieve 1000 times the system capacity, 10 times the spectral efficiency, energy efficiency, data rate and 25 times the average cell throughput. This translates to a peak data rate of 10 Gb/s for low mobility and peak data rate of 1 Gb/s for high mobility scenarios. The table ?? below shows the comparison between 2G, 3G, 4G and 5G cellular communication system.

Table 2.1: Cellular Technologies Comparison between different generations of deployed digital cellular networks. Data rates, standard and implementation technology is compared for the 3G, 4G and 5G

3G	4G	5G
1990/2002	2000/2010	2010/2022
2 Mbps WCDMA, CDMA-2000	200 Mbps – 1 Gbps (low mobility) Unified Long Term Evolution (LTE) standard	10 Gbps and higher (low mobility) In-progress

2.1 5G Cellular Architecture

The base station density is increasing drastically due to the huge spike in the use of heterogeneous networks to support massive exchange of information over the air. The heterogeneous networks are already standardized in 4G but the architecture is not natively designed to support them. The huge network densification requires major changes in the cellular architecture of 5G communication system. Wireless users mostly stay indoors for about 80% of the time, while only 20% of the mobile users stay outdoors [26]. The conventional cellular architecture consists of an outdoor base station in the middle of a cell communicating with mobile users irrespective of the user's location. Since the signal incur a large penetration loss since it has through go through buildings, thus restricting the data rates, spectral and energy efficiency of the wireless transmissions. The key idea behind 5G cellular communication is to separate the outdoor and indoor scenarios so that the penetration loss and shadowing caused by buildings can be avoided. This will be achieved by using distributed antenna system (DAS) and massive MIMO technology (also referred to as "Large-Scale Antenna Systems") where spatially located antenna arrays with hundreds of

antenna elements are deployed. Using large number of antenna arrays in base station renders the channels to the different devices quasi-orthogonal and very simple spatial multiplexing procedures quasi-optimal. The favorable action of the law of large numbers smoothens out frequency dependencies in the channel and thus leads to huge gains in the spectral efficiency [27]. The BSs deployed outdoors will be equipped with massive MIMO distributed around the cell and connected to the BS via optical fibers as a backbone network. The outdoor mobile users are normally equipped with very limited number of antenna elements, but the devices can form a virtual massive MIMO links to increase the capacity and spectral efficiency. The Figure 2.1 shows the proposed heterogeneous 5G cellular architecture by C. Weng, et.al [28].

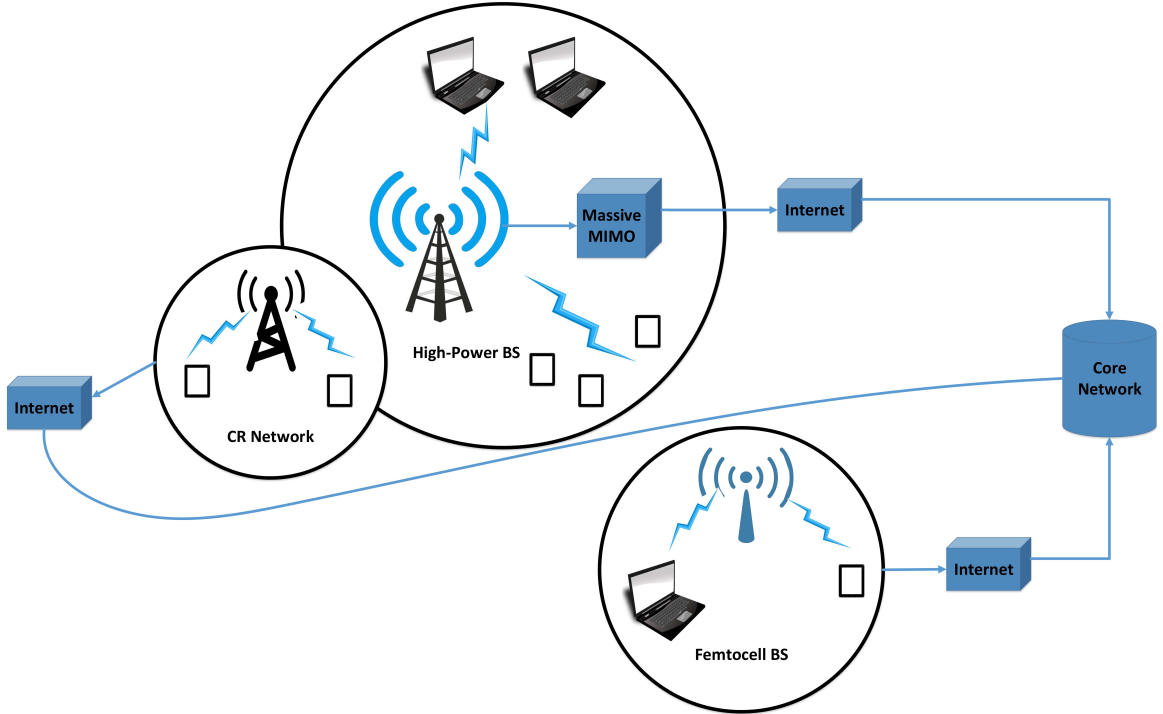


Figure 2.1: 5G Architecture

The proposed 5G cellular architecture consists of macrocells, microcells, small cells and relays. In this type of network, mobile users can be offloaded to nearby femto base stations instead of all competing for macro cells to increase the data rates per user. The massive MIMOs will be deployed outside of the buildings and will be connected to the wireless access

points inside the building via cables for indoor users. The initial startup cost for the 5G infrastructure will be very high but it will vastly improve the cell throughput, spectral efficiency and data rate of the cellular system in the long run. By separating the cellular architecture into indoor and outdoor scenarios, with indoor users only requiring to communicate with indoor wireless access points many technologies can be utilized for short-range communications with massive data rates. The examples of short-range communications system include high speed Wi-Fi, ultra wideband (UWB) , mm-wave communications (3–300 GHz) [29] and visible light communications (VLC) (400–490 THz) [30]. The backbone networks of 5G will move from copper and fiber to mm-wave wireless connections enhancing cooperation and connectivity between base stations. It is worth noting that mm-Wave and light communication systems use higher frequencies not traditionally used for cellular technologies. Using mm-Wave frequencies currently saturated radio spectrum band from 700 MHz to 2.6 GHz can also be augmented for wireless communications. The 28 GHz and 60 GHz bands are currently available with spectrum allocations of over 1 GHz of band-width. Originally intended for Local Multipoint Distribution Service (LMDS) use in the late 1990's, these licensees could be used for mobile cellular as well as backhaul [31]. These sub tera-hertz frequency waves do not penetrate solid building walls very well and can readily be absorbed or scattered by gases, rain, and foliage. The path-loss at 60 GHz at 1m distance is around 68 dB and at 10 m distance path-loss is 88 dB. Therefore, it is hard to use these waves for outdoor and long distance applications. However, with large bandwidths available, mm-Wave and visible light communication technologies can greatly increase the transmission data rate for indoor scenarios. Besides using mm-Wave and VLC, dynamic spectrum access (DSA) can also be utilized to solve the spectrum scarcity problem. The important characteristics of DSA systems is their ability to exploit knowledge of their spectral environment to adapt and modify their operational parameters to efficiently access the spectrum [32]. The key promises of these systems are that they open up the possibility of highly flexible and efficient management and reuse of spectrum across all its dimensions. The cognitive radio [33], build on software-defined radio is the intelligent, adaptive and frequency agile wireless devices that will underlie most forms of future DSA systems. In this thesis, we have implemented the cooperative spectrum sensing using software-defined radios which are uti-

lizing the spatial gain to improve the accuracy of primary user detection. The primary user detection is very important factor in utilizing the spectrum efficiently so we don't interfere with the incumbent users. The heterogeneous networks has already been introduced in 4G LTE architecture but their use has been very limited and but due to rapid densification of wireless devices 5G cellular architecture should be a heterogeneous one. In the following sections we will discuss the some key technologies which will drive the advancement of 5G cellular system.

2.2 Key Technologies of 5G System

To understand the engineering challenges facing 5G cellular communication, it is paramount to first identify its requirements. The following items are requirements in each key dimension, but it is important to note that all of these need to be satisfied simultaneously to achieve bounds set for 5G technology. Due to the rapid advancement in IoT devices different applications will place different requirements on the performance of the network. Applications with high data rate for e.g., streaming high-definition videos may have relaxed latency and quality of service (QoS) requirements compared to driverless cars or public safety applications, where latency QoS are paramount but lower data rates can be tolerated. Before we get into the key features of 5G cellular system, we first need to classify the impact of new technologies and their implications for 5G. These new technologies are classified leveraging the Henderson-Clark model and are as follows [?]:

- New changes are required at both the node and architectural level, for e.g. the introduction of codebooks and signaling support for a large number of antennas (Massive-MIMO).
- Complex changes in the design of network nodes are required, for e.g. introduction of new waveforms. These are the modifications required at the component level.
- The heterogeneous architecture of 4G system will act as a good benchmark for future 5G systems, but we need disruptive changes in the 5G system architecture.
- To achieve data rates in the order of tens of gigabits with much lower latency cannot be

achieved by merely building on the current system architecture, we need to completely redesign the system at node and component level.

Some key features for the 5G wireless system which we think will be important in revolutionizing the cellular radios for the massively dense wireless devices in the future.

2.2.1 Massive MIMO

Massive (Very Large) multiple-input multiple-output MIMO Systems is a multiple antenna technology which is becoming ready for wireless communications and has been implemented for wireless broadband standards like LTE and Wi-fi. The key idea behind using large number of antennas is to create more possible signal paths and to achieve better performance in terms of data rate and link reliability via spatial multiplexing [34]. Figure 2.2 describes the implementation of massive MIMO technology using the patch antenna arrays communicating with several user equipments (UE). The implementation is proposed for the 5G system as the patch antenna arrays can be mounted on the walls of the buildings due to their thin size and can provide high-speed data rate coverage in outdoor environment also.

Massive MIMO Patch Antenna

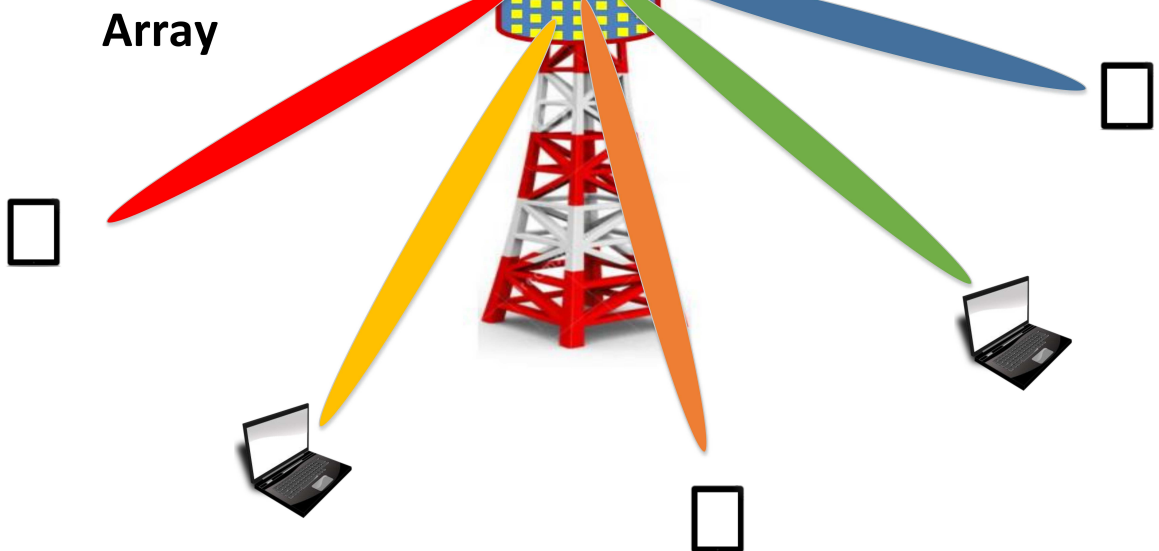


Figure 2.2: Massive-MIMO implementation using patch antenna arrays

Massive-MIMO is the key technology for 5G cellular system and it has a clear distinction from the existing LTE/4G system through the use of a very large number of service antenna that can operate adaptively and in a fully coherent manner. It proposes utilizing a very high number of antennas to multiplex data signals for several UEs on each time-frequency resource, focusing the beam toward the intended directions while minimizing intra- and inter-cell interference. Using hundreds and thousands of antennas help in focusing the beam in a smaller regions of space, thus bringing huge improvements in throughput, gain and energy efficiency. This can particularly help in bringing large improvement when combined with simultaneous scheduling of a large number of UEs. Figure 2.3 shows the beamforming using $N = 4, 8, 12$ and 16 antenna elements using linear dipole arrays. The antenna array gain for $N = 4, 8, 12, 16$ is 9.23 dB, 12.3 dB, 14.1 dB and 16.15 dB respectively. By using hundred or thousands of antenna array element we can achieve a very high gain and throughput. Massive MIMO may require major architectural changes, particularly in the design of macro base stations, and it may also lead to new types of deployments.

Using Massive-MIMO in 5G system will also lead to making extensive use of inexpensive low-power components, low latency and simplification of media access control (MAC) layer. Although with the arrival of massive-MIMO many traditional problems have become irrelevant, it opens up an entirely new areas research in 5G system. While a very promising technology, massive-MIMO still presents a number of research challenges which need to be addressed. Acquisition of channel state information (CSI) is critical and currently represents the main source of limitations. The mobility of users imposes a finite coherence interval during which channel knowledge must be acquired and utilized, and consequently there is a finite number of orthogonal pilot sequences that can be assigned to the devices [27]. There is still a lot of research which need to be conducted in massive-MIMO propagation, some experiments thus far have supported the hypothesis of channels being quasi-orthogonal. Synchronization is also very important issue for large number of antenna arrays with the need for reduced power consumption. These are some of the issues which need to be taken care of, for the next generation cellular system.

From above discussion, it can be concluded that implementation of massive-MIMO for 5G cellular system could represent an important breakthrough and major leap with respect

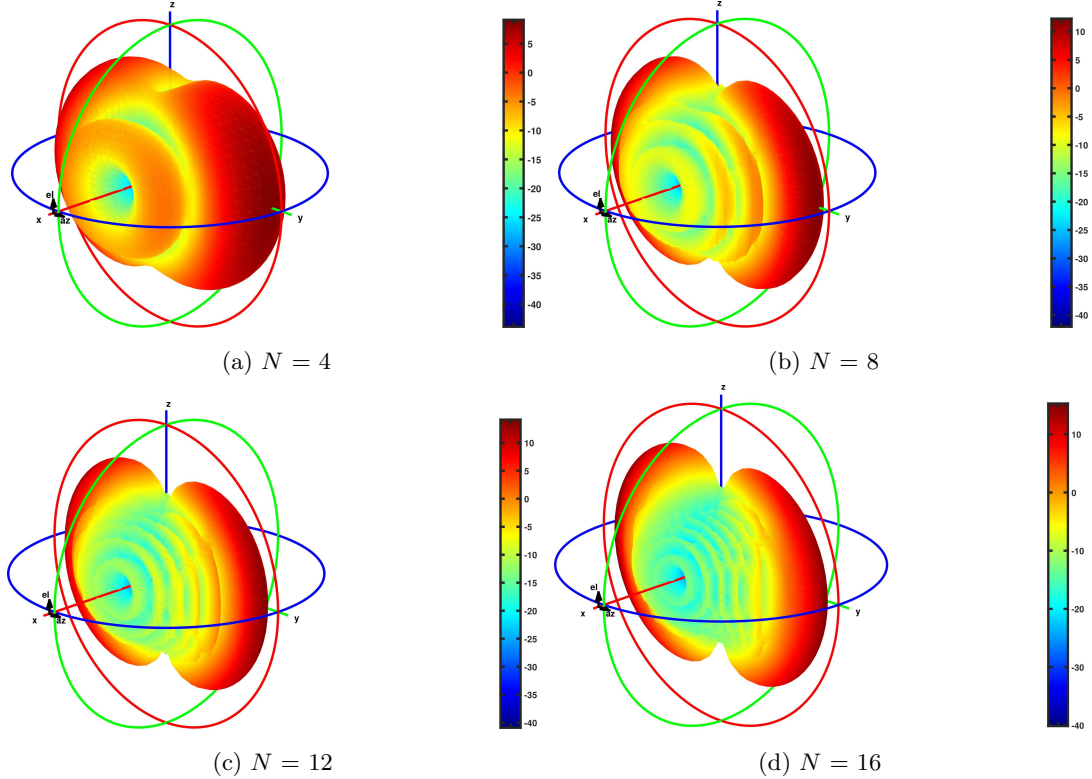


Figure 2.3: Beamforming for $N=4, 8, 12$ and 16 linear dipole antenna elements. As the number of antenna element increases we see a sharper beam confined in a smaller region. Massive-MIMO can utilize beamforming to increase spatial gain and spectral efficiency.

to the current state-of-the-art in cellular technology. These modifications at system level needs to be justified for its massive infrastructure cost by solving the challenges currently faced by this key technology via simulations and test-bed experimentations.

2.2.2 Machine-to-Machine (M2M) Communication

Machine to machine (M2M) communication is a new paradigm proposed to be a key technology in 5G wireless systems that enables the ubiquitous connectivity between a set of devices with different network stack. Thus, the autonomous connection of devices facilitates the emergence of a wide range of intelligent M2M applications. M2M exhibits a strong potential to improve human life in different fields such as e-Health, smart grids, smart cities, intelligent transportation and surveillance enabling internet of things (IoT) applications.

A native inclusion of M2M communication in 5G involves satisfying three fundamentally different requirements associated with different classes of low data rates and power consumption services such as: enabling massive number of low-rate devices simultaneously, a minimal data rate in virtually all scenarios, even in worst fading environment and finally managing the above two requirements with a very low latency.

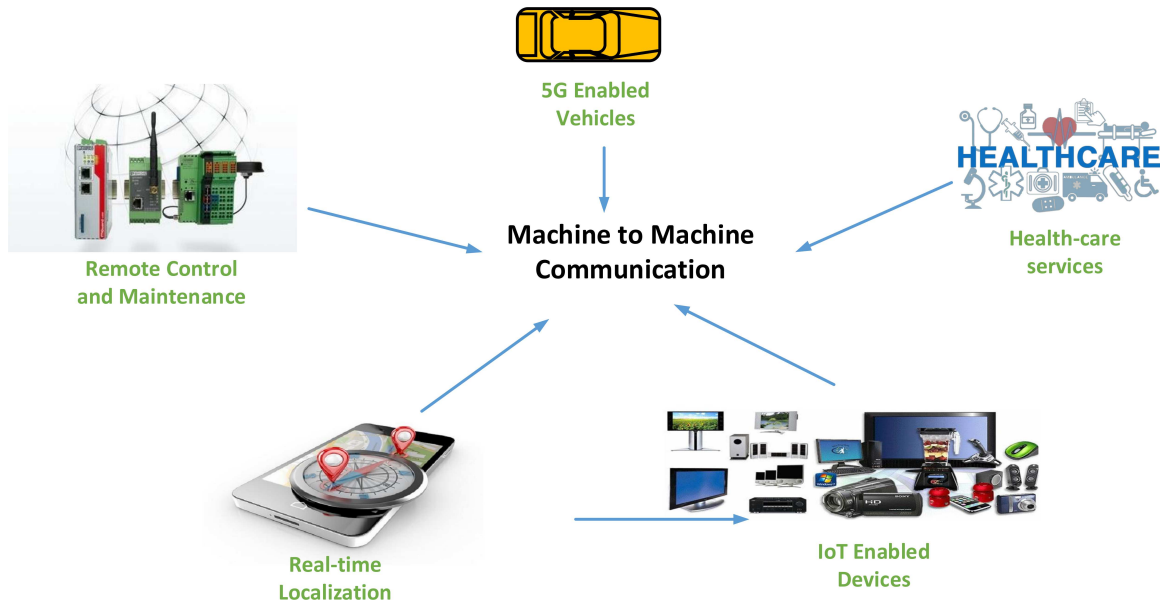


Figure 2.4: Machine-to-Machine communication paradigm in 5G Cellular System.

Implementing these requirements for 5G system, new communication paradigms needs to be developed at network and physical layer. Figure 2.4 shows the machine-to-machine communication and how it helps in integrating devices which can be used in health care, localization, vehicular communication, remote maintenance and consumer electronics. In the future standardization of the 5G networks, the M2M communication is recognized as one of the key technologies that will support the 5G architecture. As a consequence of this proliferation of M2M technology, large numbers of devices will produce huge amount of irregular data and significantly higher capacity of cellular networks will be needed, in terms of spectrum, power control as well as the number of devices serviced simultaneously. For next generation 5G system, it would be common to have situations where devices will be in close proximity to each other and would like to wirelessly share data like videos, im-

ages, etc. or would like to interact for gaming, social networking. If these communication scenarios are handled by simply connecting through the network it can lead to various inefficiencies at various levels. The reason is that cellular networks were primarily designed to support mobile devices with a large amount of data to transmit, whereas most M2M communications are duty-cycling and delay-tolerant with small data packets between stationary terminals [35]. Thus, connecting a massive number of M2M devices directly with cellular networks will saturate uplink traffic easily [36]. In this context, non-cellular connections should serve as important supplement and extension to cellular networks. Some of the challenges of connecting the devices via cellular networks are:

- Multi-hopping is used to reach destination which otherwise requires fundamentally a single hop. This entails a multi-fold waste of signaling resources as well as higher latency.
- Huge amount of transmit power is consumed in uplink(fraction of a watt) and down-link(several watts) for data communication which can be easily achieved by milli-watts of power. This leads to unnecessary levels of battery drainage and interference to all other devices occupying the same signaling resources in near proximity.
- Propagation path-losses to the base stations are much stronger than direct link to the device, hence the corresponding spectral inefficiencies are also lower.

It is pretty evident that M2M has huge potential to handle single hop inter device communication more efficiently but these task could be offloaded to other radio access technologies such as Bluetooth, ultra-wide band (UWB) or Zigbee. The applications requiring a mixture of low-latency and high data rates for e.g. interaction between users via augmented reality could be more apt for 5G M2M communication system. In particular, machine-to-machine is as an important enabler for applications requiring low latency, especially in future network deployments utilizing baseband centralization and radio virtualization. There are still various research challenges which need to be taken care of before we can integrate this technology in 5G cellular communication system. The devices for M2M communication need to be designed from both hardware and protocol perspective by providing the needed

flexibility at both the PHY and MAC layers. Research needs to be conducted for possible extra overheads for control and channel estimation and also accessing of true net gains associated with M2M mode. And finally, accurate simulation and experimental test-beds needs to be designed for testing M2M communication.

2.2.3 Spectrum Regulation for 5G

Departing from technical issues, we now discuss the crucial interactions that 5G will encounter with spectrum policy and allocation by the federal communications commission (FCC). As already discussed in Section 2.1 the spectrum allocated for cellular technologies is already saturated in peak markets due to massive amounts of wireless services and networks. Figure 2.5 shows the pronounced scarcity in the the wireless cellular bands as seen in the FCC frequency allocation chart. Large amount of unused spectrum is available in the mm-Wave realm and can be used for high data rate applications. Due to different propagation characteristics for signals at low and sub-terahertz frequencies, future systems will need to integrate a broad range of frequencies. Frequencies on a lower spectrum can be used for wide coverage, mobility support, control signaling and high frequencies for high data rate applications in small cells. This requires a new approach to spectrum policy and allocation methods for 5G standardization.

Cognitive radio is a promising technology that can solve the spectrum shortage problem arising due to the rapid increase in wireless networks and mobile devices. Recent advancements in software-defined radio technology and edge computing have enhanced the cognitive radio network (CRN) capabilities and, along with some adjustments in its operation, will be a key technology for 5G heterogeneous network deployment. The CR network is an innovative software-defined radio technique considered to be one of the key technologies to improve the utilization of the congested radio spectrum [37]. Integrating CR technology into 5G system is motivated by the fact that a large portion of the radio spectrum is underutilized most of the time. For achieving data rates in order of gigabits per second, we need to make an efficient use of available spectrum which can be achieved by utilizing CRNs. In CR networks, a secondary system can share spectrum bands with the incumbent primary system, either on an interference-free basis or on an interference-tolerant basis. The CR network should

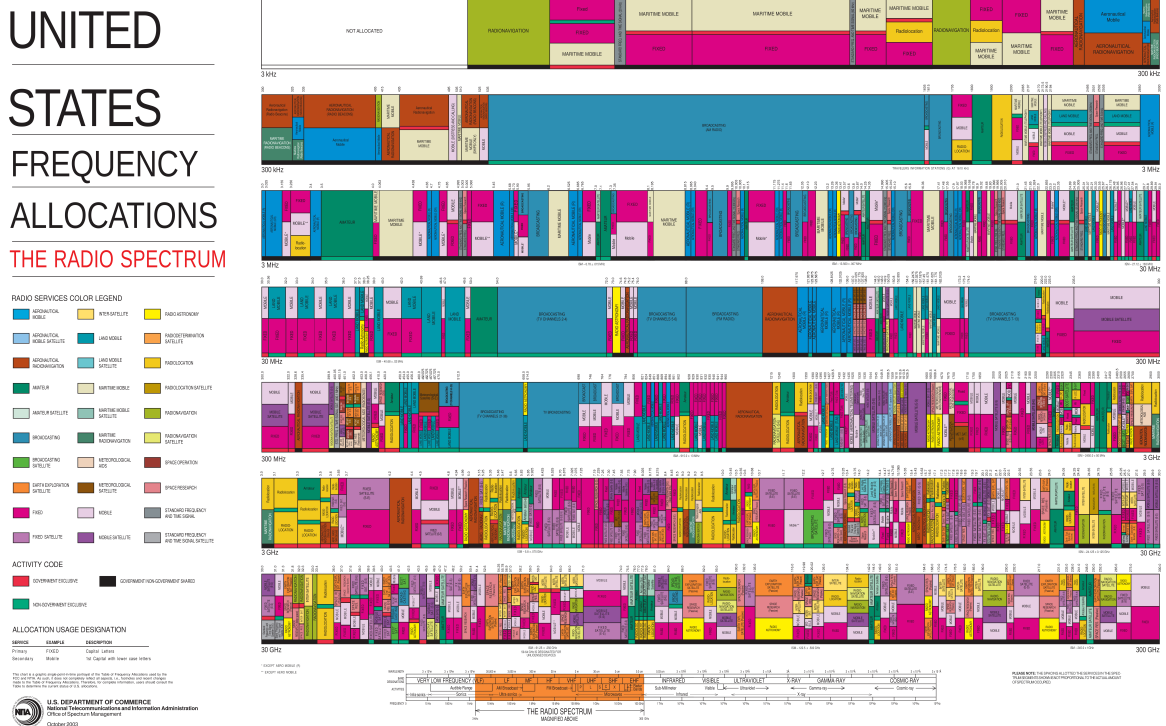


Figure 2.5: Machine-to-Machine communication paradigm in 5G Cellular System.

be aware of the surrounding radio environment and regulate its transmission accordingly. In interference-free CR networks, CR users are allowed to borrow spectrum resources only when licensed users do not use them. A key to enabling interference-free CR networks is figuring out how to detect the spectrum holes (white space) that spread out in wideband frequency spectrums and facilitate dynamic spectrum access (DSA) smoothly [38].

CR receivers should first monitor and allocate the unused spectrum via spectrum sensing (energy detection (ED), covariance absolute value (CAV) detection, etc.) or combining with geolocation databases and feed this information back to the central CR controller. A coordinating mechanism is required in multiple CR networks that try to access the same spectrum to prevent users colliding when accessing the matching spectrum holes. In interference-tolerant CR networks, CR users can share the spectrum resource with a licensed system while keeping the interference below a threshold. In comparison with interference-free CR networks, interference-tolerant CR networks can achieve enhanced spectrum utilization by opportunistically sharing the radio spectrum resources with licensed users, as well as better

spectral and energy efficiency. However, it has been shown that the performance of CR systems can be very sensitive to any slight change in user densities, interference threshold, and transmission behaviors of the licensed system. However, the spectral efficiency can be improved by either relaxing the interference threshold of the primary system or considering only the CR users who have short distances to the secondary BS (utilizing the spatial gain). Hybrid CR networks have been proposed in [39] for adoption in cellular networks to explore additional bands and expand the capacity. CR networks can only prove beneficial if the spectrum policies related to 5G are implemented in a robust manner.

2.3 5G using Millimeter Wave (mmWave)

The massive growth in wireless traffic has drawn an increased attention to the large amount of underutilized spectrum in the mm-Wave frequency bands as a possible solution for achieving gigabits of speed as promised for 5G implementation. Current spectrum for cellular radio (under 5 GHz) is congested and using CR network it can be made more efficient, but for 5G cellular system it is still better to go for bands above 10 GHz. A vast amount of largely unused spectrum is available and can be utilized for 5G. Wireless community has earlier ruled out mm-Wave for cellular usage due to the high penetration loss and its limited usage for short-range communications. And there was also the concern that rain and atmosphere make mm-Wave spectrum useless for mobile communications. The former problem is solved by dividing the cellular architecture into outdoor and indoor environment so that high-data rate applications can be implemented for direct line-of-sight (LOS) communication. As for latter when one considers the fact that todays cell sizes in urban environments are on the order of 200 m, it becomes clear that mm-wave cellular can overcome these issues [29]. In [40] recent results from channel measurement campaigns and development of advanced algorithms, a prototype is discussed in details which makes mm-Wave band a worthy candidate for next generation 5G cellular system.

Concerns regarding the propagation characteristics at higher frequencies such as higher penetration, precipitation, and foliage losses are legitimate even though the actual amounts of additional propagation losses vary depending on the material of the building, the strength

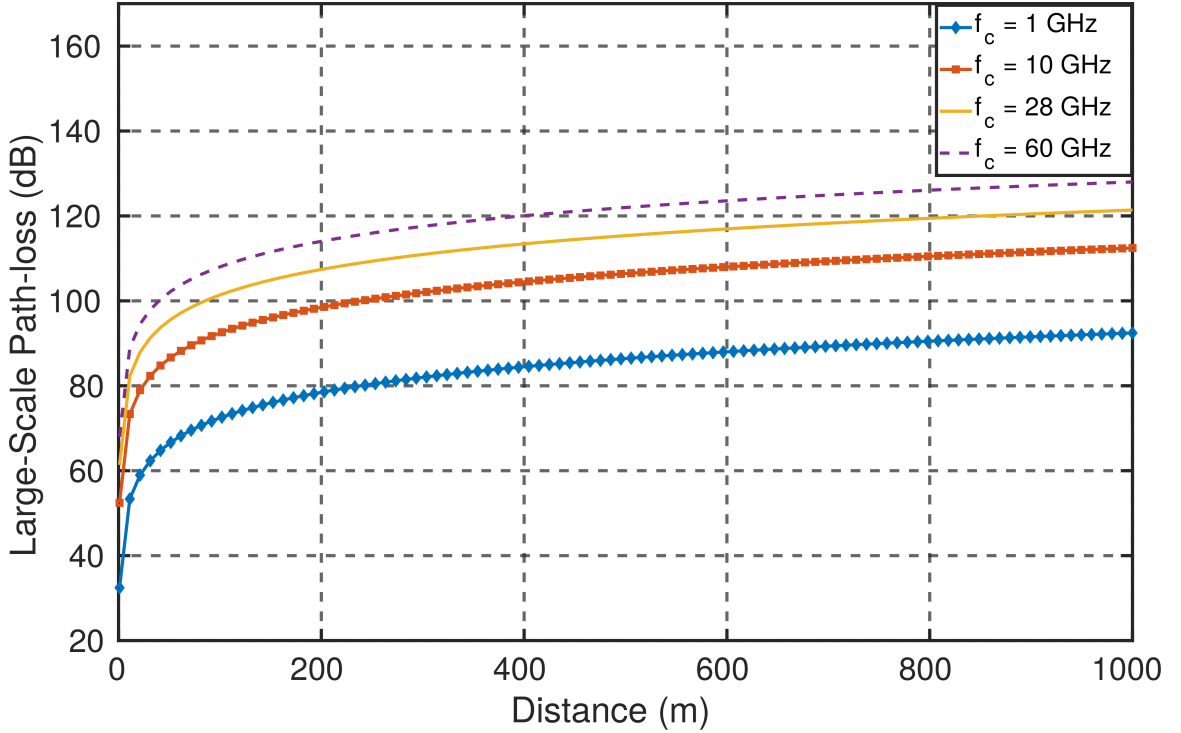


Figure 2.6: Large-scale propagation loss for $f_c = 1 \text{ GHz}$, 10 GHz , 28 GHz and 60 GHz .

of rain, or the thickness of foliage. Figure 2.6 shows the large-scale propagation loss for different frequencies and as we can see that as we go higher in frequencies, path-loss increases for an isotropic antenna. The plot also shows that after certain distance the propagation losses almost saturates and doesn't deteriorate as sharply as they do in first 10 meters. The most common misunderstanding, however, of the propagation characteristics at higher frequencies is that they always incur a much higher propagation loss even in free space compared to lower frequencies, and thus are not adequate for long-range communications. In [29] they have conducted laboratory measurements using a patch antenna at 3 GHz and an array antenna at 30 GHz of the same physical size within an anechoic chamber. And their results shows same amount of propagation loss regardless of the operating frequency when an array antenna of the same physical aperture size is used at the 30 GHz receiving end. And additionally they also showed when array antennas are used at both transmitting and receiving ends at 30 GHz, the measured receive power is 20 dB higher than that of the 3 GHz patch antenna case. To understand how the path-loss is same for 3 GHz and 30 GHz

frequencies let's start with friis equation.

$$P_r = P_t + G_t + G_r + 20 \log \left(\frac{c}{4\pi df} \right) \quad (2.1)$$

where P_r is the received power in free space, P_t is the transmit power, G_t , G_r are transmit and receive antenna gains, respectively, d is the distance between the transmitter and receiver in meters, f is the carrier frequency and c is the speed of light. From Eq.(2.1) it is pretty evident that received power is inversely proportional to the frequency squared for an ideal isotropic antenna. However, in reality antennas or an antenna arrays have gains of G_t and G_r greater than 1 and are typically employed at both ends. The most important factor for advocating mm-Wave is that antenna gains are proportional to the frequency squared given a fixed physical aperture size [41]. Given the same physical aperture size, therefore, transmit and receive antennas at higher frequencies, in fact, send and receive more energy through narrower directed beams, which is not commonly recognized. And since the physical size of antennas at mm-Wave frequencies is so small that it becomes practical to build hundreds and thousands of antennas elements to provide huge gains from spatial isolation and multiplexing for 5G cellular communication system.

2.4 Vehicular Communication Using 5G

With the development of mm-Wave and massive-MIMO, the spectral and energy efficiency for 5G wireless communications has been drastically improved. The development of driverless cars has posed some rigorous requirements for the safety of the passengers and pedestrians. For safety-critical applications the transmission delay needs to be less than 1 ms which is required for intelligent transportation systems (ITSs) and vehicular networks [42]. Considering the drawbacks of IEEE 802.11p networks, such as poor scalability, low capacity , and intermittent connectivity, the Long Term Evolution (LTE) mobile communication technologies were proposed to support vehicular applications [43]. Simulation and experiment results revealed that there is a trade-off between the proposed performance metrics and system parameters, such as base station (BS) and vehicle densities, radio coverage, and the maximum number of hops in a path. When LTE communication technologies

have been integrated into vehicular networks, the interference has cut down the performance of LTE vehicular networks. When vehicle density is high, the beaconing signals of vehicular safety applications may easily overload the serving eNodeB. To handle this issue, a significant amount of such signals should be distributed directly among vehicles, without going through the eNB. In LTE-Advanced (LTE-A), device-to-device (D2D) communication is considered to allow direct message delivery between terminals in proximity to lighten the load of eNB [44].

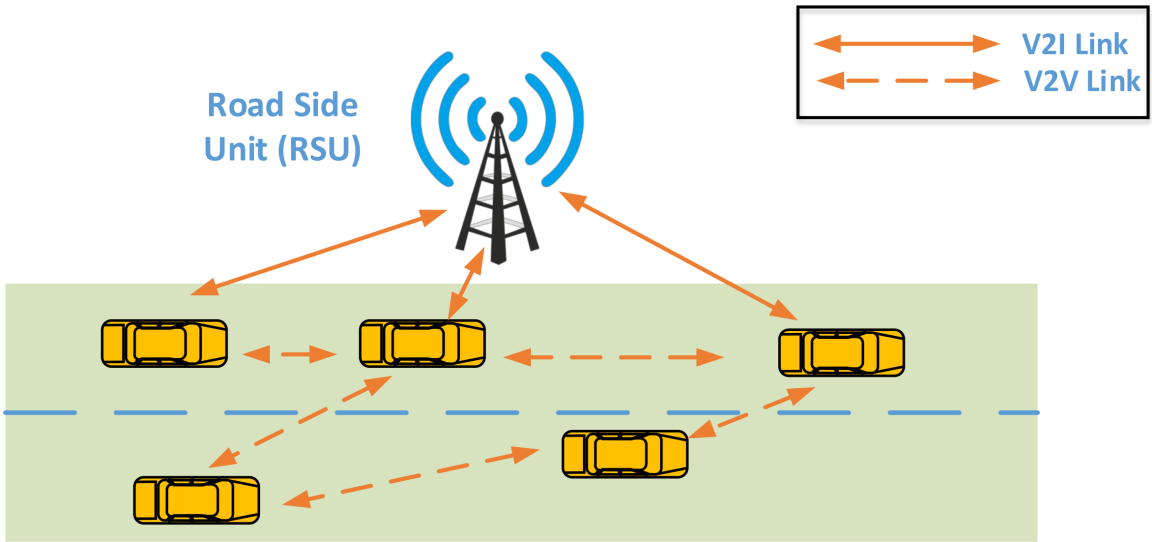


Figure 2.7: Vehicular communication using D2D 5G cellular communication technology.

Hence the infrastructure-aided D2D technologies can serve as a natural approach to enable reliable and efficient V2V communications without negatively affecting existing cellular systems. To meet the high performance requirements, such as low transmission delay and high throughput, a new architecture for 5G vehicular communication is required. Figure 2.7 describes the vehicular communication using D2D communication strategy where significant amount of computation is offloaded from road side units (RSU) to vehicles to avoid increase spectral and efficiency. The communication environment in V2V is quite different than in D2D due to high mobility (Doppler shift) of vehicles. Network connectivity play a important role in V2V communication than D2D, compared with system throughput. These features can significantly affect D2D resource allocation strategies and system parameters, and thus

should be modified for vehicular communication.

2.5 Summary

Summary will go here for now use this demo msg CR receivers should first monitor and allocate the unused spectrum via spectrum sensing (energy detection (ED), covariance absolute value (CAV) detection, etc.) or combining with geolocation databases and feed this information back to the central CR controller. A coordinating mechanism is required in multiple CR networks that try to access the same spectrum to prevent users colliding when accessing the matching spectrum holes. In interference-tolerant CR networks, CR users can share the spectrum resource with a licensed system while keeping the interference below a threshold. In comparison with interference-free CR networks, interference-tolerant CR networks can achieve enhanced spectrum utilization by opportunistically sharing the radio spectrum resources with licensed users, as well as better spectral and energy efficiency. However, it has been shown that the performance of CR systems can be very sensitive to any slight change in user densities, interference threshold, and transmission behaviors of the licensed system. However, the spectral efficiency can be improved by either relaxing the interference threshold of the primary system or considering only the CR users who have short distances to the secondary BS (utilizing the spatial gain). Hybrid CR networks have been proposed in [39] for adoption in cellular networks to explore additional bands and expand the capacity.

Chapter 3

Heterogeneous Cooperative Spectrum Sensing (CSS)

This chapter provides the background information needed to understand the chapters that follows. It examines the basic outlines of a heterogeneous networks and how cooperative spectrum sensing (CSS) can help in enhancing the accuracy of signal source estimation. The fusion center (FC) collects the data from the sensor node network and process it to make the reliable decision. Secondly, this chapter investigates various algorithms which can be used in heterogeneous network to estimate signal source. Finally, it also outlines the necessary hardware and software tools used in the implementation of heterogeneous CSS chapter.

3.1 Cognitive Radios

Cognitive radio (CR) [45] is a communication systems paradigm that focuses on employing highly agile, environmentally aware, intelligent wireless platforms in order to autonomously select and configure device operating parameters based on the prevailing radio and network environmental conditions [3]. In general the cognitive radio may be expected to look at parameters such as channel occupancy rate, available channels, bandwidth required for data transmission and the modulation types that may be used. It must also look at the regulatory requirements set by the Federal Communications Commission. In

some instances a knowledge of geography and this may alter what it may be allowed to do. Software-defined radios (SDR) are mainly responsible for making cognitive radios used in wireless communications system a reality. Software radios provide a vast untapped potential to personalize services, and they make the process of modifying the radio characteristics extremely simple.

The work is underway to determine the best possible methods of developing the cognitive radio communications system that can fulfill all its requirements. To facilitate the intelligent decision making capabilities in these cognitive radio systems, machine learning algorithms have been proposed in the literature [46–49] to automate the reconfiguration process. The Figure 3.1 describes the various building blocks of a cognitive radio system. The spectrum sensing is performed to estimate the spectrum holes in the band and after the analysis the decision strategy is prepared. The radio is configured with the new parameters based on the radio environment and the spectrum decision made.

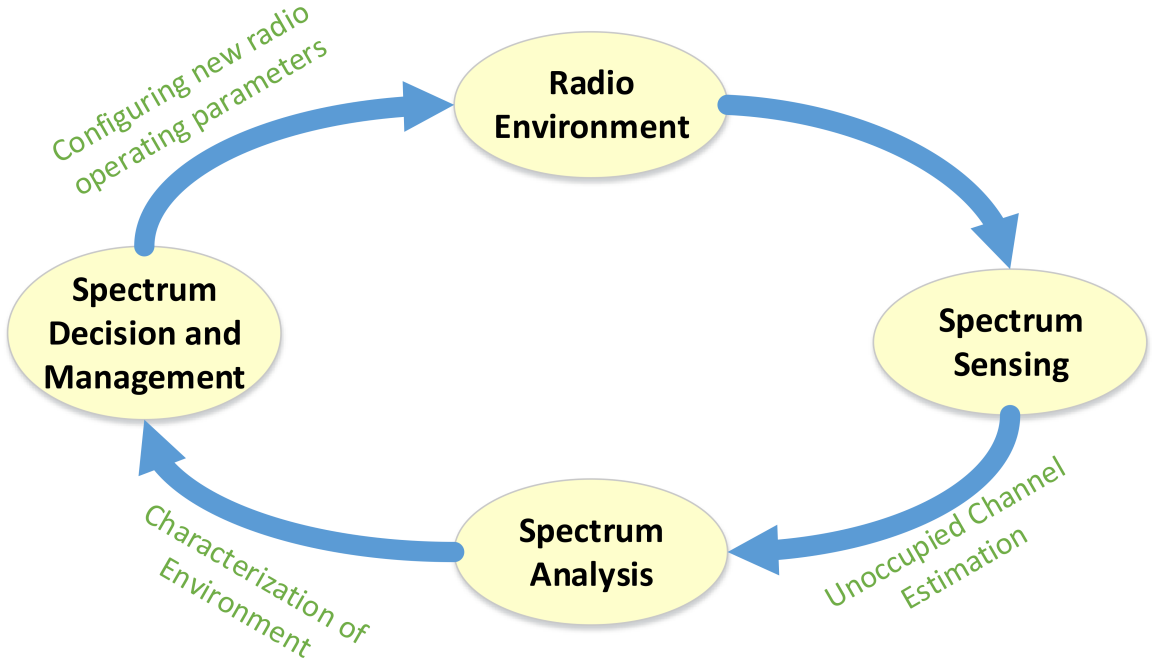


Figure 3.1: The block diagram explaining the basic parts of Cognitive Radio system. The operating parameters are configured based on the characterization of the wireless environment.

3.2 CSS in Heterogeneous Networks

In Heterogeneous CR network, each radio is equipped with different numbers of antennas, sampling rates and RF characteristics. In addition, each sensor node may experience distinct channel fading and suffer from different noise levels due to their respective locations and device performances, such as amplifier and ADC. As a result, each node may have different sensing capabilities and reliability values. This is a universal and fundamental characteristic of a heterogeneous CR network which requires robust algorithms to achieve high accuracy in signal source detection for estimating the presence of a primary user [50]. In this thesis, we investigate the cooperative spectrum sensing in heterogeneous networks with a centralized FC, a transmitter acting as a signal source and four sensor nodes. As explained earlier we are using energy detection as one of the spectrum sensing technique since it possesses a very low implementation complexity [4]. The energy detection scheme detects the presence or absence of a signal source based on its intercepted energy signature. If the energy of the signal is higher than a certain threshold, this indicates that the channel is occupied. The ED can be modeled by the equation:

$$y(n) = \begin{cases} w(n), & \mathbf{H}_0 \\ s(n) + w(n), & \mathbf{H}_1 \end{cases} \quad (3.1)$$

where $y(n)$ represents the received signal, $s(n)$ represents the signal source PU, and $w(n)$ is the white Gaussian noise $w(n) \sim N(0, \sigma_n^2)$. \mathbf{H}_0 describes the hypothesis when there is no signal present, while the hypothesis \mathbf{H}_1 is the presence of signal.

The decision whether the signal is present or absent is decided by evaluating a local test statistic L to see whether it is above or below certain fixed threshold τ . The local test statistic L , which is the complex-magnitude squared of the FFT samples, is compared with τ using equation:

$$L = \sum_{n=1}^M |y(n)|^2 = \begin{cases} < \tau, & \mathbf{H}_0 \\ > \tau, & \mathbf{H}_1 \end{cases} \quad (3.2)$$

where $|y(n)|^2$ is the energy of a specific FFT bin and $n=1,2,3\dots M$ are the number of samples received.

The probability of false alarm P_{fa} and probability of detection P_d are given by:

$$P_f = Q\left(\frac{\tau - M(2\sigma_n^2)}{\sqrt{M(2\sigma_n^2)}}\right), \quad (3.3)$$

$$P_d = Q\left(\frac{\tau - M(2\sigma_n^2)(1 + \gamma)}{\sqrt{M(1 + 2\gamma)(2\sigma_n^2)}}\right). \quad (3.4)$$

In cooperative spectrum sensing, each sensor node transmits the local sensing data to the fusion center for signal source detection. The local sensing data has to be quantized, thus yielding quantization errors. To minimize the quantization error in local test statistic L and to reduce the effect of noise variance, the energy of the received signal $y(n)$ is normalized [50].

The local test statistic L for the r^{th} sensor node is given as:

$$L_r = \frac{1}{M_r \sigma_{n,r}^2} \sum_{r=1}^{M_r} |y(n)|^2 \quad (3.5)$$

where M_r is the number of samples used to estimate the power of the signal source in the node, $\sigma_{n,r}$ is the noise power variance.

In Eq (3.1) $s(n)$ is considered as a deterministic signal and $w(n)$ is a Gaussian random variable with a variance of σ_n^2 . Based on CLT, L_r will have a following distribution [7]:

$$L_r = \begin{cases} N(1, \frac{1}{M_r}), & \mathbf{H}_0 \\ N(\gamma_r + 1, \frac{1 + 2\gamma_r}{M_r}), & \mathbf{H}_1 \end{cases} \quad (3.6)$$

where γ_r is the received SNR of the r^{th} SU. The local decision statistic L_r is quantized before transmission due to the bandwidth constraint, and this can lead to quantization errors. The values of L_r received by FC can be modeled as:

$$\beta_r = L_r + w_{q,r}, \quad (3.7)$$

where β_r is the decision statistic received by the FC and w_q is the noise added to the signal due to fading and quantization error. In [51], the w_q is modeled as a Gaussian noise with zero mean and σ_q^2 variance.

3.3 Software Defined Radios

We have already explained about the cooperative spectrum sensing in heterogeneous networks, now in this section we will look at the platform for testing the CSS algorithms. The platform which we use is a new hardware frontier called Software-Defined Radio (SDR) and is discussed in details.

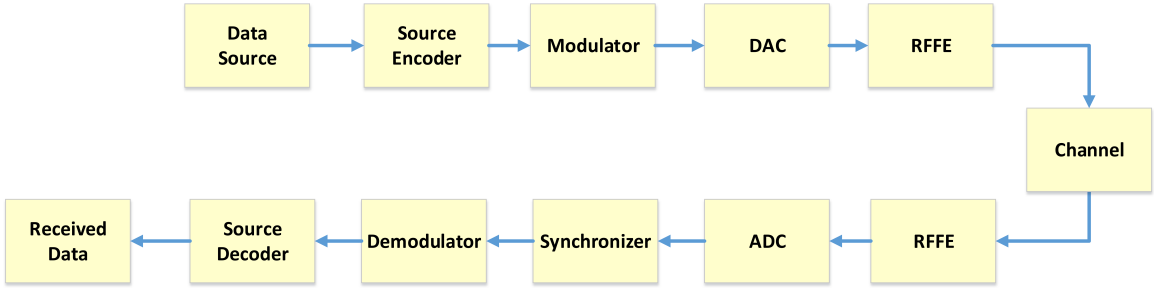


Figure 3.2: Software defined radio pushes all the adaptive elements and data manipulation operation into software. The goal of SDR is to provide or define all of the radio operation in software.

There has been a huge shift in the definition of a Software-Defined Radio and it has a lot to do with the question of where the hardware ends and software begins. Dr. J. Mitola III coined the Software Defined Radio which he described as a of digital signal processing (DSP) primitives, a meta-level system for combining the primitives into communication system (Tx, channel model, Rx, etc.), functions and a set of target processors on which the software radio is hosted for real-time communications [52]. Dr. J. Mitola explains in the paper how software provides the flexibility which using hardware alone can never be achieved. And as time progresses SDR would become more dominant and close to ideal Cognitive Radio system.

The SDR technology existed since the 1970s but the key milestone in the advancement of SDR technology took place in early 1990s with the U.S. military initiative called SpeakEasy I/II. The SpeakEasy project was implemented to use programmable processing to emulate more than ten existing military radios, operating in frequency bands between 2 MHz and 2 GHz [53]. With SpeakEasy the operator could talk to ten radios operating under different

standards with any hardware modifications. With all these features, unfortunately there were some shortcomings which left much to be desired. The device was large enough to fit on the back of a pickup truck [53] which is good for ground station but not if the mobility is an important factor. And in 1992 the field programmable gate arrays (FPGA) were not computationally efficient, hence required large time to change their operating characteristics. The two software-defined radios we used in the thesis are Universal Software Radio Peripheral (USRP N210) and RTL-SDR R2832U. In the subsequent subsections we discuss the two SDRs in detail.

3.3.1 Universal Software Radio Peripheral (USRP) N210 and RTL-SDR

The USRP N210 has a very different RF characteristics compared to RTL-SDR hence modeling an ideal heterogeneous network. The USRP N210 provides a very high bandwidth, dynamic range processing capability. The product architecture includes a Xilinx Spartan 3A-DSP 3400 FPGA [54], 100 MS/s dual ADC, 400 MS/s dual DAC and gigabit ethernet connectivity to stream data to and from host processors. A modular design allows the USRP N210 to operate from DC to 6 GHz, while an expansion port allows multiple USRP N210 series devices to be synchronized and used in a MIMO configuration. An optional GPSDO module can also be used to discipline the USRP N210 reference clock to within 0.01 ppm of the worldwide GPS standard. The USRP N210 can stream up to 50 MS/s to and from host applications. Users can implement custom functions in the FPGA fabric, or in the on-board 32-bit RISC softcore. The USRP N210 provides a larger FPGA than the USRP N200 for applications demanding additional logic, memory and DSP resources. The FPGA also offers the potential to process up to 100 MS/s in both the transmit and receive directions. The FPGA firmware can be reloaded through the Gigabit Ethernet interface [22].

RTL-SDR is a very cheap software defined radio that uses a DVB-T TV tuner dongle based on the RTL2832U chipset. With the combined efforts of Antti Palosaari, Eric Fry and Osmocom it was found that the signal I/Q data could be accessed directly, which allowed the DVB-T TV tuner to be converted into a wideband software defined radio via a new software driver. Essentially, this means that a cheap \$20 TV tuner USB dongle with the RTL2832U chip can be used as a computer based radio scanner. This sort of scanner

capability would have cost hundreds or even thousands of dollars just a few years ago. The RTL-SDR is also often referred to as RTL2832U, DVB-T SDR, RTL dongle or the \$20 Software Defined Radio.

3.3.2 GNURadio and Software-Defined Radio

The first software package to be discussed by this thesis is GNU Radio. GNU Radio provides the reconfigurable signal processing blocks that are necessary for software defined radios. GNU Radio is an open source project allowing for SDR developers to develop unique signal processing blocks and SDR systems. GNU Radio was started in 2001, originally forked from the SpectrumWare project developed at the Massachusetts Institute of Technology [46]. Since 2001, the code base has undergone massive changes, containing almost no code from the original SpectrumWare project. Physically the code consist of three languages Python, C++, and SWIG. Python provides the overarching control of the system or program, while C++ provides the actual signal processing blocks and mathematics. SWIG is a wrapper for C++ which allows Python to dynamically wrap around C++ and control or compile with it. A diagram below better illustrates this architecture. It is also important to mention that there as significant paradigm shifts in the community, pushing more and more code to Python rather than C++, due to its easier programming syntax and structure.

GNU Radio provides a very structured framework of flow design. Data processing segments are extremely self contained to minimize error propagation during system debugging. Since the software is open-source full access to all code is provide, giving low-level access to all operation within GNU Radio. Much of the actions have been abstracted to limited the knowledge of the lower layers, but if specific actions are required for an application. Then serious depth or knowledge is needed about the overall projects structure, which is quite overloading.[Travisthesis]

3.3.3 MATLAB

MATLAB is an extremely well known engineering, mathematical, biological, and financial software suite. MATLAB provide massive data leverage and advanced communication system models and algorithm for significant data processing. Since 2007, they have also

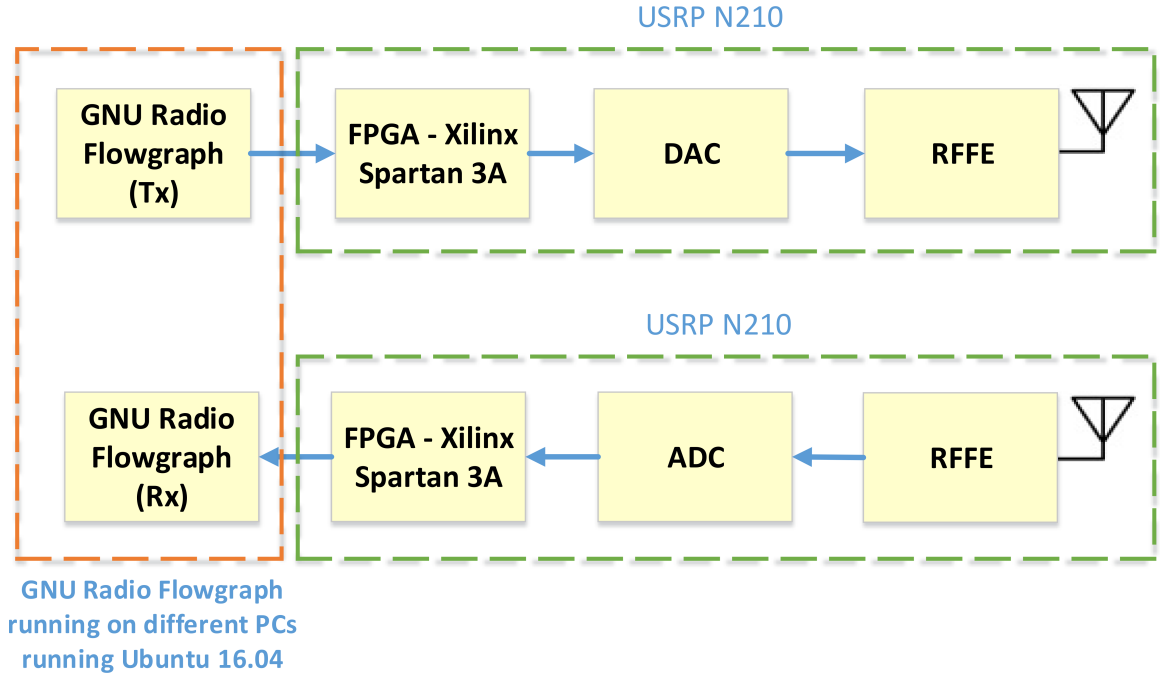


Figure 3.3: GNURadio and Software-Defined Radio

provided hardware compliance with specific SDR platforms through their Simulink platform, and more recently within MATLAB itself [47]. This thesis primarily utilizes the signal processing and communication system aspects of MATLAB, since MATLAB cannot fully utilize all aspects of the chosen hardware. It is important to note under alternate constraints, MATLAB can provide adequate performance directly interfacing with hardware, especially when accessing its targeting features seen here [48]. Figure shows an example of a common MATLAB SDR model through Simulink.[Travis]

3.4 Summary

This chapter outlined and examined the topics of jamming and anti-jamming techniques, and provided a foundation in communication system theory and advanced equalizer design. Secondly it setup an understanding of Software-Defined Radio, the power of such an architecture, and examples of implementations and existing software for future designs. Next, this thesis will consider a new anti-jamming technique and design an implementation of

such a system. After the implementation is investigated, the result of specific experiments on such an implementation will be analyzed.

Chapter 4

Long Term Evolution for Railways (LTE-R)

4.1 LTE-R Communication System

LTE-R System Description To provide improved and more efficient transmission for HSR communications, it is vital to consider frequency and spectrum usage for LTE-R. HSRs are important strategic infrastructure, and, in some countries, this argument is being leveraged to convince governments that large spectrum chunks need to be allocated specifically for it. Some industry bodies, including the European Railway Agency (ERA), China Railway, and UIC, are working to secure spectrum allocation for HSR use. Currently, most LTE systems work at the bands above 1 GHz, such as 1.8, 2.1, 2.3, and 2.6 GHz, although 700900-MHz bands are also used in some countries. Large bandwidth is available in the upper bands, giving a higher data rate, whereas lower frequency bands offer longer distance coverage. Figure 1(b) summarizes the possible frequency bands for LTE-R in China, Europe, and Korea. As a high-frequency band has larger propagation loss and more severe fading, the radius of an LTE-R cell would be $\sqrt{2}$ km [due to the strict requirement of signal-to-noise ratio (SNR) and BER in HSR], leading to frequent handovers and a requirement of substantial investment for higher BS density. Therefore, the low-frequency bands, such as 450470 MHz, 800 MHz, and 1.4 GHz, have been widely considered. The 450470-MHz band is already

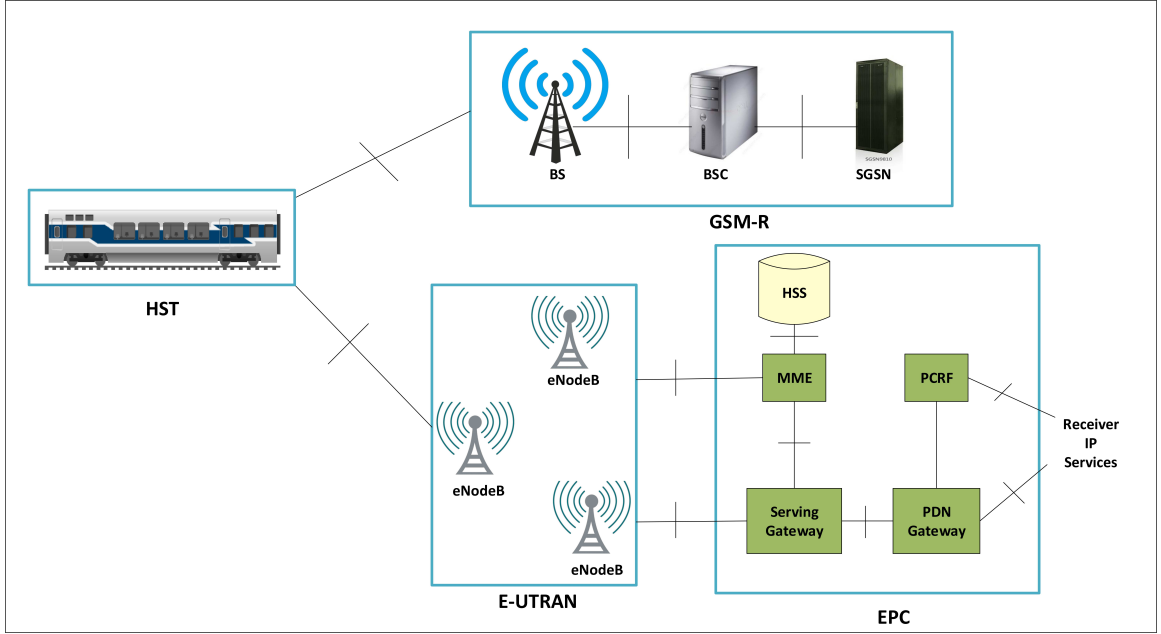


Figure 4.1: High speed train inside a tunnel for LTE-R. D_{LOS} is the distance between transmitter and receiver, d is the distance between the LCX cable transmission slots.

well adopted by the railway industry; therefore, dedicated bandwidth for professional use can still be allocated from local regulators. Furthermore, the carrier aggregation capability of LTE will permit the use of different bands to overcome problems of capacity. Figure 1(b) presents the detailed frequency allocation of 450–470 MHz in China [12], and it is feasible to allocate enough bandwidth for LTE-R within this band. In Europe, the FRMCS of UIC would like to build on the current GSM-R investment by reusing the existing mast sites, which could save as much as 80–90% of the cost of a network. Railways are also concerned about continuing to make use of their GSM-R masts, and, therefore, a spectrum allocation under 1 GHz is more cost effective in Europe. However, the selection of frequency band depends on government policy and differs by country.

Standard LTE includes a core network of evolved packet core (EPC) and a radio access network of Evolved Universal Terrestrial Radio Access Network (E-UTRAN). The Internet protocol (IP)-based EPC supports seamless handovers for both voice and data to cell towers, and each E-UTRAN cell will support high data and voice capacity by high-speed packet access (HSPA). As a candidate for the next-generation communication system of HSR, LTE-

R in- herits all the important features of LTE and provides an extra radio access system to exchange wireless signals with onboard units (OBUs) and to match HSR-specific needs. The future architecture of LTE-R according to [4] is pre- sented in Figure 2, and it shows that the core network of LTE-R is backward compatible with GSM-R.

Compared with the public LTE networks, LTE-R has many differences, such as architecture, system parameters, network layout, services, and QoS. The preferred parameters of LTE-R are summarized in Table 1, based on the future QoS requirements of HSR communications. Note that LTE-R will be configured for reliability more than capacity. The network must be able to operate at 500 km/h in complex railway environments. Therefore, quadrature phase-shift keying (QPSK) modulation is preferred, and the packet number of retransmission must be reduced as much as possible.[RuisiHeBoAiGongpuWang/HSRCommunications]

4.2 Leaky Coaxial Cable

Substantial work has been done for the radio communication in tunnel environments.

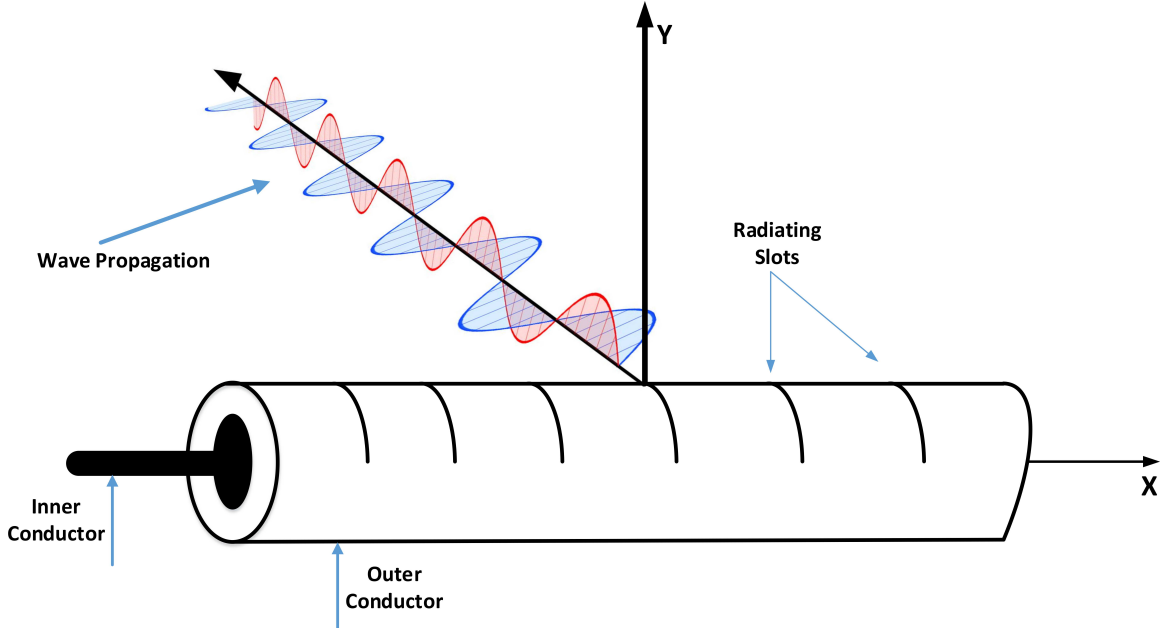


Figure 4.2: Leaky Coaxial Cable

Authors of [2]measure the radio channel frequency response; the large scale and small

scale fading in tunnel are investigated through field experiments. Statistical characteristics of the propagation channels are suggested in [3]. Both [2] and [3] indicate that WLAN cannot achieve good performance when used in tunnel environments. As a result, leaky waveguide and leaky coaxial cable are used in wireless communication due to their stability and robustness from the interference. The availability of train ground communication in subway systems by waveguide is analyzed in [4] and [5]. Meanwhile, leaky coaxial cable is also studied. H. Cao [7] introduces the way to calculate frequency range of LCX and shows experimental results about LCX performance at 1.8GHz. Authors of [11] introduce the propagation at 2GHz in an enclosed area using a leaky coaxial cable. Authors of [12] study the theory of leaky coaxial cable with periodic slots, and frequency band of the studied LCXs is from 450MHz to 900MHz. However, few people specialize in the performance of leaky coaxial cable at 2.4GHz band, especially the application in tunnels.[Hongwei Wang Bin Ning and Hailin Jiang]

4.3 Channel Impairments Inside a Tunnel

The tunnel environment is affected by multipath and diffraction effects due to multiple reflections from the tunnel walls, which leads to a substantial fading environment. By deploying LCX cables, we can eliminate the large penetration loss due to tunnel walls. However, small-scale fading can still cause a large amount of errors and decrease the QoS for the communication link.

High velocity trains experience very high Doppler shifts and a fast fading channel. These problems can lead to significant BER degradation of the LTE system. The frequency shifts caused by the Doppler phenomenon can lead to shifts in the sub-carrier frequencies for OFDM, which leads to synchronization errors. The maximum Doppler shifts for a train traveling at 500 km/h is 2.314 kHz for a 5 GHz carrier frequency. This large Doppler shift can also lead to significant drops in the quality of wireless signals and increase the bit error rate. Thus, to develop an efficient and reliable communication link inside tunnels, we need to properly model this channel impairment and build our proposed channel model by taking into account these tunnel phenomena. These impairments are described in detail in the

following subsections.[OwnPaper]

4.3.1 Multipath Fading

The following time-varying multipath channel impulse response considers the effects of Doppler shift and scattering [11]: where τ is the path delay, t is time in seconds, $[h_k(t)]$ is the impulse response, f_c is the carrier frequency, $h_k(t)$ is the envelope of the time-varying channel and consists of both large and small-scale fading components. Since the structure of LCX is almost the same as a leaky waveguide, the large scale fading of channel can be modeled linearly [8]. There is also no signal shadowing and the line-of-sight (LOS) signal component is always present along the tunnel. This type of channel fading can be best described by a Ricean fading model. The probability density function $p()$ of a Rician fading model is given by [10]: where K is the Rician factor and a is the complex amplitude of the channel response function that has a unity second moment.

4.3.2 Doppler Shift

The 3GPP channel model [14] is used for its Doppler shift profile in high speed railway environment. The measurements obtained for the Doppler frequency shift are implemented for two scenarios. The first scenario is for an open space while the second scenario is for high speed trains. Doppler shift is not taken into consideration. There exists a third scenario for tunnels using multiple antennas. Since the slots of LCX can be modeled as multiple antenna system, we use this Doppler shift profile for our proposed channel. The Doppler shift variation $f_s(t)$ is described by

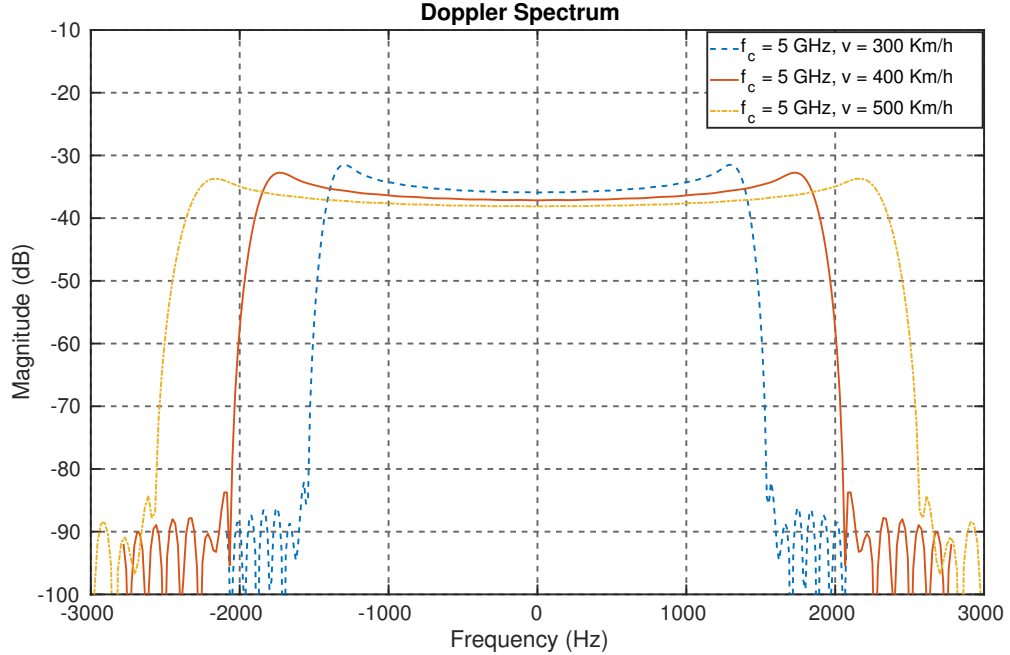


Figure 4.3: Doppler spectrum for LTE-R at different train velocities v (km/h) = 300, 400 and 500 and $f_c = 5$ GHz.

4.4 Two-Ray Propagation Model

4.4.1 Classical Two-Ray Propagation Model

4.4.2 Dynamic K-factor

4.5 Summary

This chapter outlined and examined the topics of jamming and anti-jamming techniques, and provided a foundation in communication system theory and advanced equalizer design. Secondly it setup an understanding of Software-Defined Radio, the power of such an architecture, and examples of implementations and existing software for future designs. Next, this thesis will consider a new anti-jamming technique and design an implementation of such a system. After the implementation is investigated, the result of specific experiments on such an implementation will be analyzed.

Chapter 5

Implementation

5.1 Overview

5.2 Experimental Setup for Heterogeneous CSS

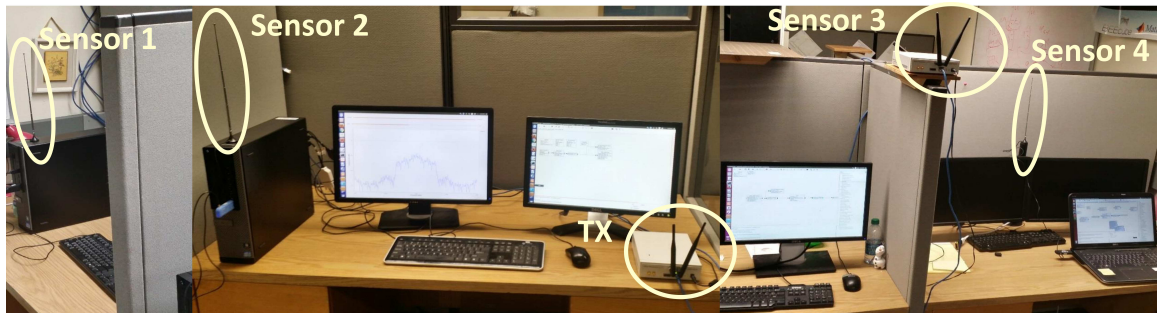


Figure 5.1: Experimental Test-Bed For Cooperative Sensing in Heterogeneous Network. Sensors 1, 2 and 4 are RTL-SDR units, sensor 3 is USRP N210 and TX is another USRP N210 unit which is used as a signal source for this work.

5.2.1 Transmitter Setup for CSS Measurements

5.2.2 Sensor Nodes Setup

The central frequency is kept at 450 MHz and the operating parameters of each sensor node is provided in the table.

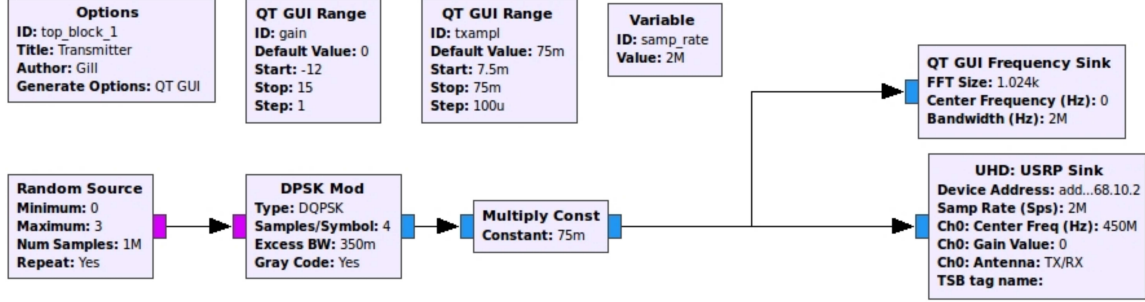


Figure 5.2: GNU Radio Flowgraph For Transmitter Running on USRP N210.

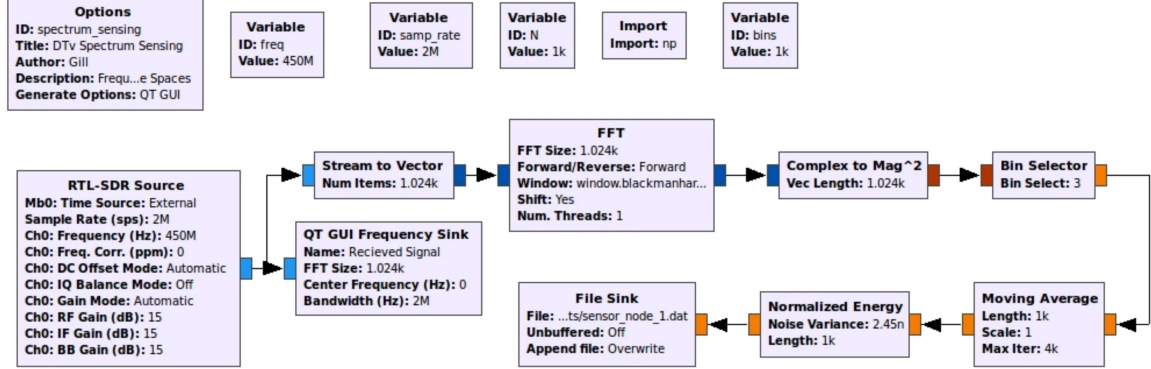


Figure 5.3: GNURadio Flowgraph For USRP and RTL-SDR sensor nodes.

Table 5.1: Operating Characteristics of Sensor Nodes

Nodes	F_s	Gain	FFT Size	Bin Size
RTL-SDR-1	1.1 Msps	10 dB	512	2.148 KHz
RTL-SDR-2	1.8 Msps	10 dB	512	3.515 KHz
RTL-SDR-3	2.4 Msps	10 dB	512	4.687 KHz
USRP N210	7.2 Msps	10 dB	512	14.062 KHz

5.3 Hard Fusion

The flowchart describes the three hard data fusion schemes.

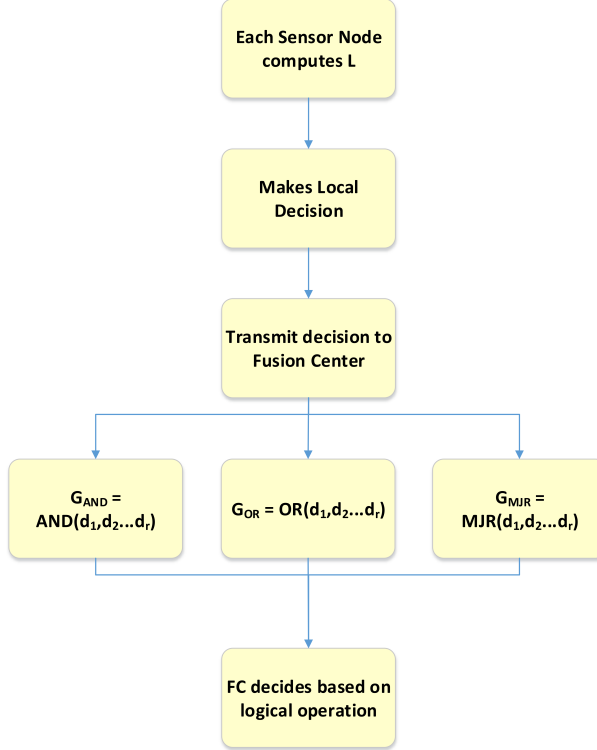


Figure 5.4: Flowchart showing AND, OR and Majority Rule Fusion schemes..

Table 5.2: Tunnel and Tx/Rx Characteristics

	Dimensions	Simulation Parameters
Tunnel	Width = 8.6 m, Height = 7.3 m	$\varepsilon_r = 5, \sigma = 0.1 \text{ Sm}^{-1}$
Leaky Feeder Cable (Tx)	Height = 6.1 m	$f_c (\text{GHz}) = 2, 3, 5$
Train (Rx)	Height = 4.2 m	$v (\text{km/h}) = 300, 400, 500$

5.4 Soft Fusion

5.4.1 Maximum Normalized Energy Scheme

5.4.2 Equal Gain Combining Scheme

5.5 LTE-R Testbed in Matlab

The below table gives the tunnel parameters which we used in the thesis for MATLAB simulaton.

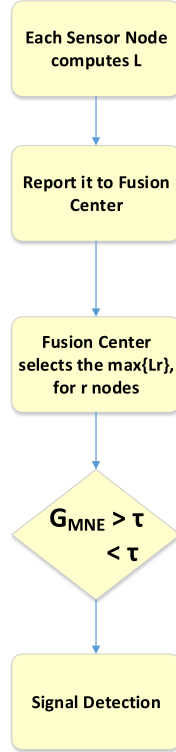


Figure 5.5: Flowchart showing Equal Gain Combining Scheme.

5.5.1 HST Channel Model

5.5.2 LTE-R OFDMA

5.6 Summary

This chapter outlined and examined the topics of jamming and anti-jamming techniques, and provided a foundation in communication system theory and advanced equalizer design. Secondly it setup an understanding of Software-Defined Radio, the power of such an architecture, and examples of implementations and existing software for future designs. Next, this thesis will consider a new anti-jamming technique and design an implementation of such a system. After the implementation is investigated, the result of specific experiments on such an implementation will be analyzed.

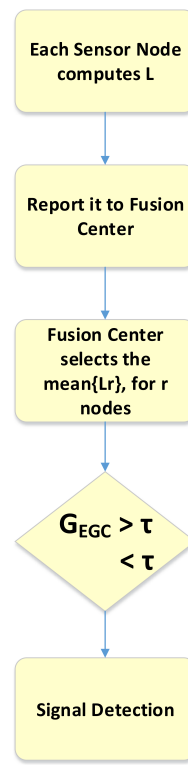


Figure 5.6: Flowchart showing Maximum Normalized Energy Scheme.

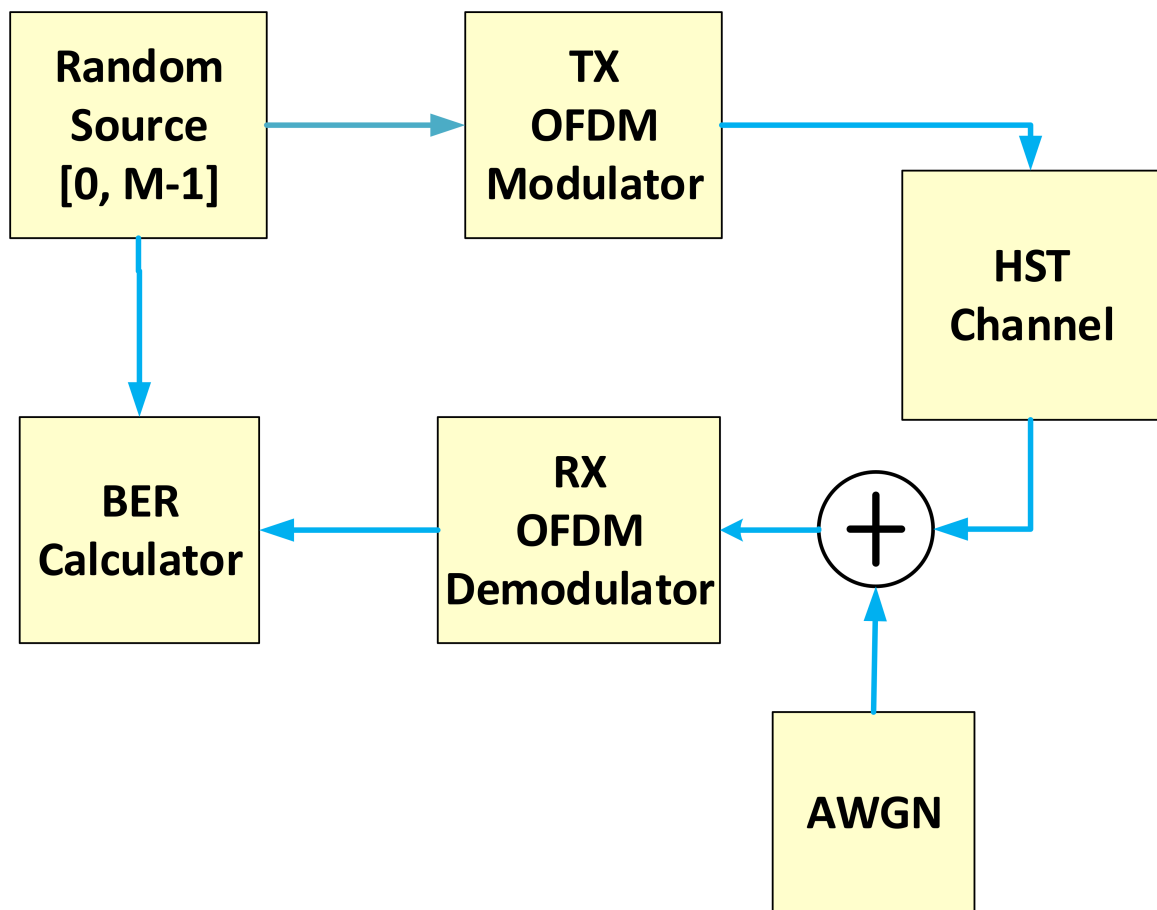


Figure 5.7: Block diagram of a communication system through a HST channel using QPSK, 16-QAM and 64-QAM.

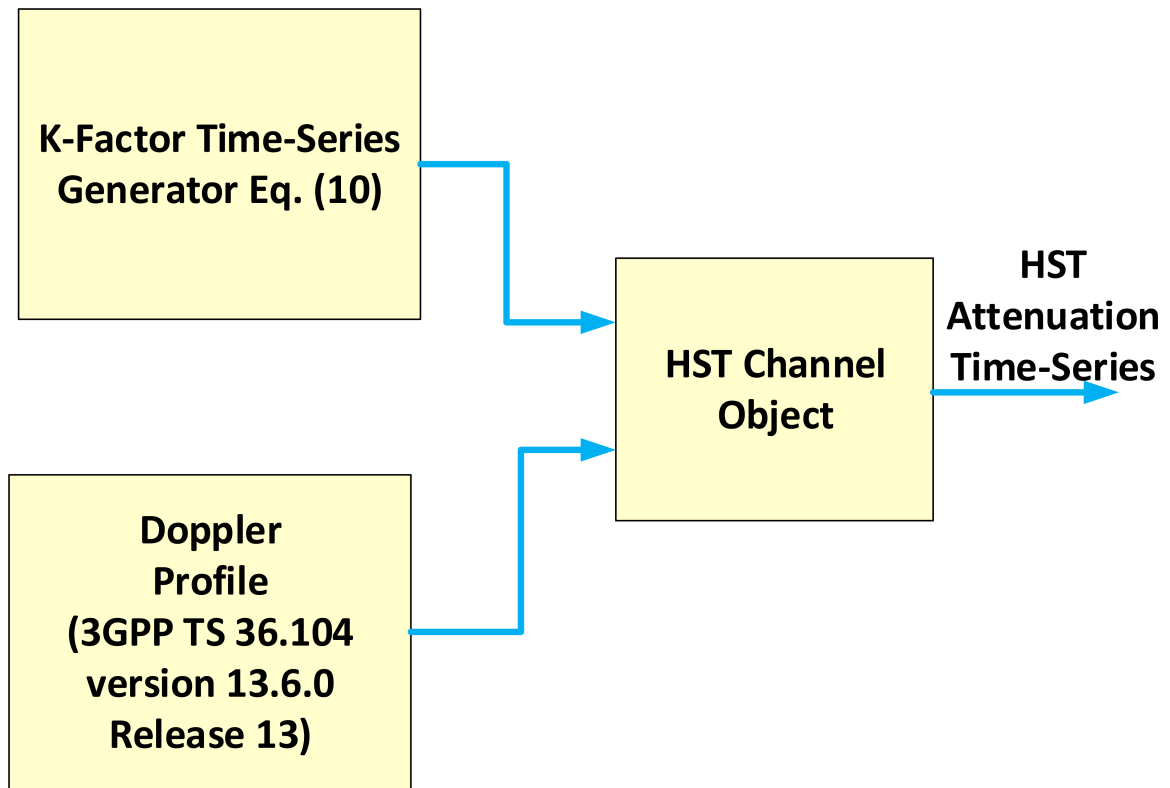


Figure 5.8: HST channel model consisting of time-series K-factor and Doppler shift caused due to velocity of the train.

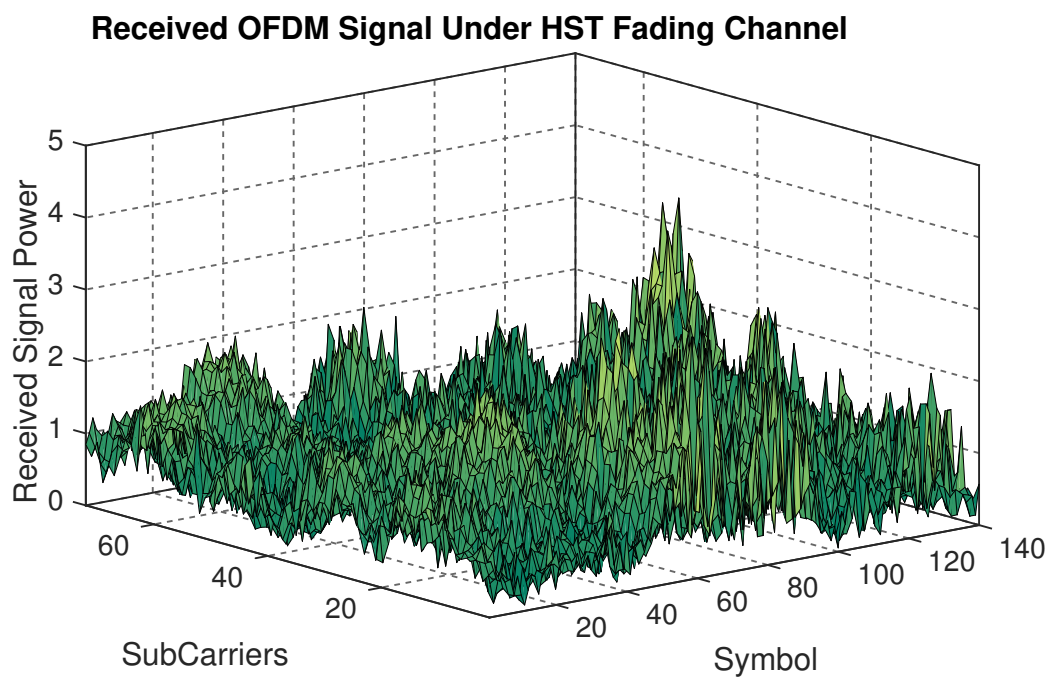


Figure 5.9: Received LTE-R OFDM signal under HST Ricean Fading Environment.

Chapter 6

Experimental Results

6.1 Overview

6.2 Heterogeneous CSS Results

6.2.1 Hard Decision Combining

6.2.2 Soft Decision Combining

6.3 HST LTE-R in a Tunnel

6.3.1 K-factor in a Tunnel

6.3.2 BER Performance

6.3.3 Real-time BER in a Tunnel

6.4 Summary

Spectral Subtraction is a extremely well studied area in signal processing, but no existing literature exists for its application in a digital communication system. It has been shown here that it can be quite difficult for it to be applied, even under strict constraints. Under the conditions of this thesis, the assumptions are quite reasonable, but due to the large amount of error in the results, more may need to be considered. These may include

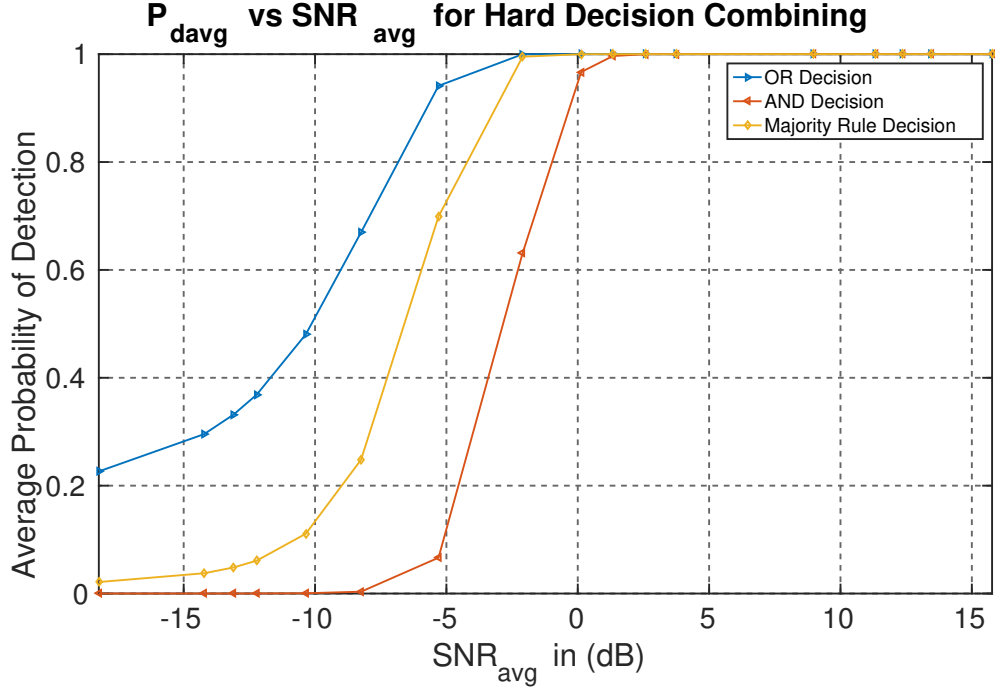


Figure 6.1: Probability of Detection versus SNR_{avg} For Hard Decision Combining.

accuracy requirements for physical equipment, primarily to reduce carrier frequency drift. Burst scenarios may also be considered to reduce bit error rate. Overall, for a completely non-existent field of study, these results point the possibility of operational success. Future work will be required, especially during the implementation phase of designs.

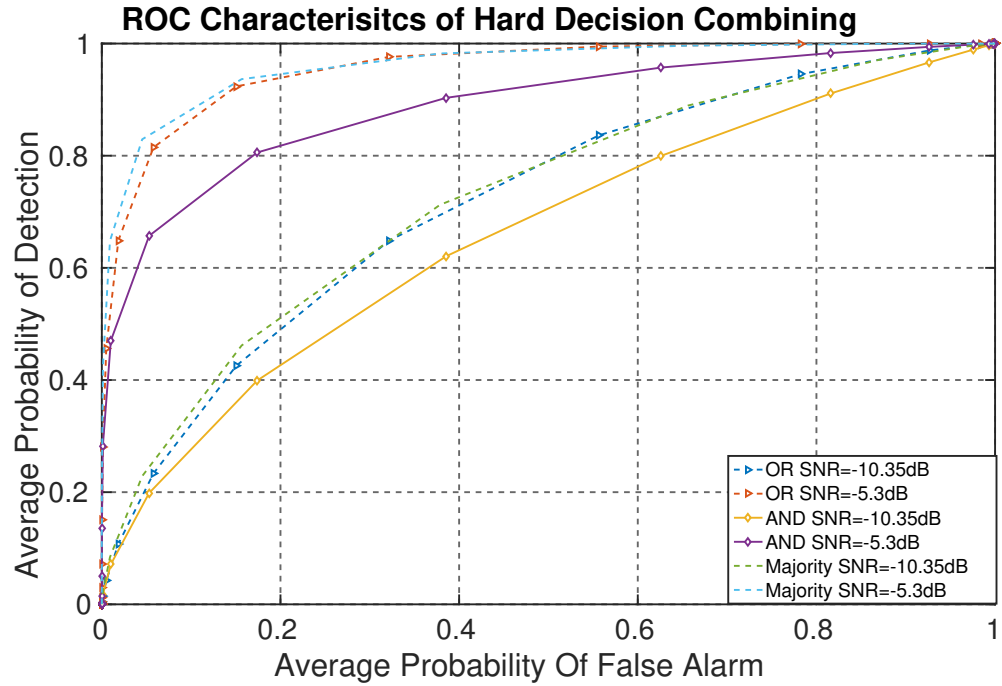


Figure 6.2: ROC Characteristics for Hard Decision Combining with Different SNRs.

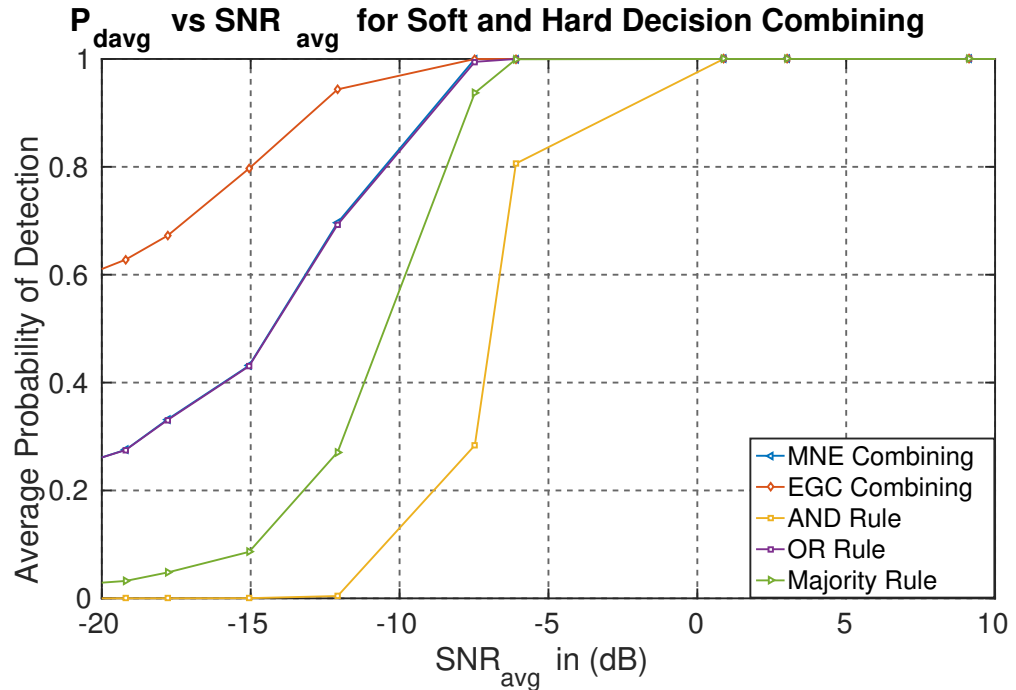


Figure 6.3: Probability of Detection versus SNR_{avg} For Soft and Hard Decision Combining.

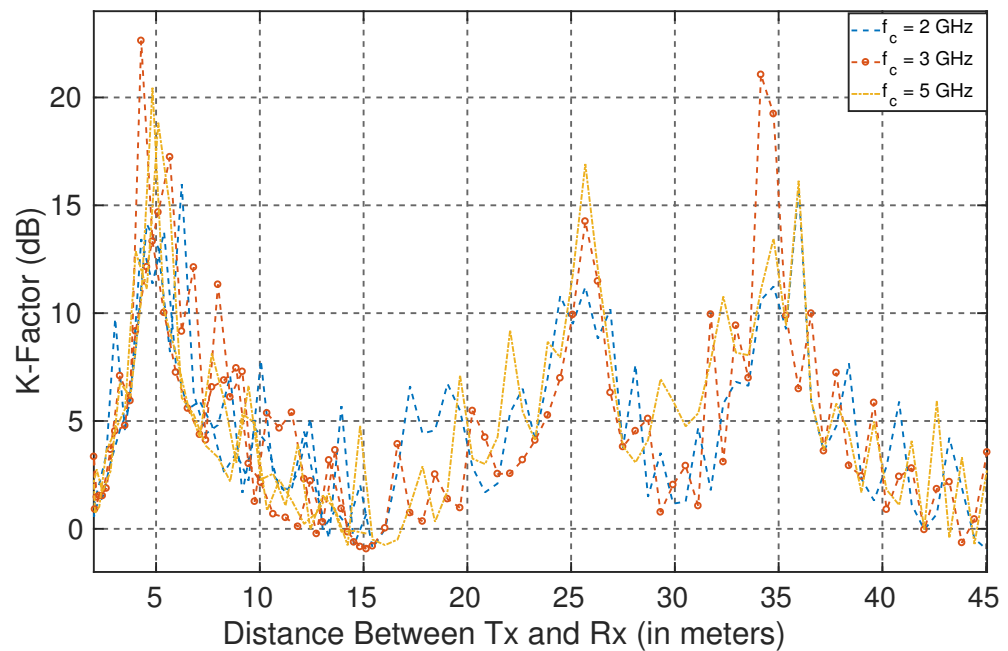


Figure 6.4: K-factor versus D_{LOS} for different center frequencies $f_c = 2, 3$ and 5 GHz .

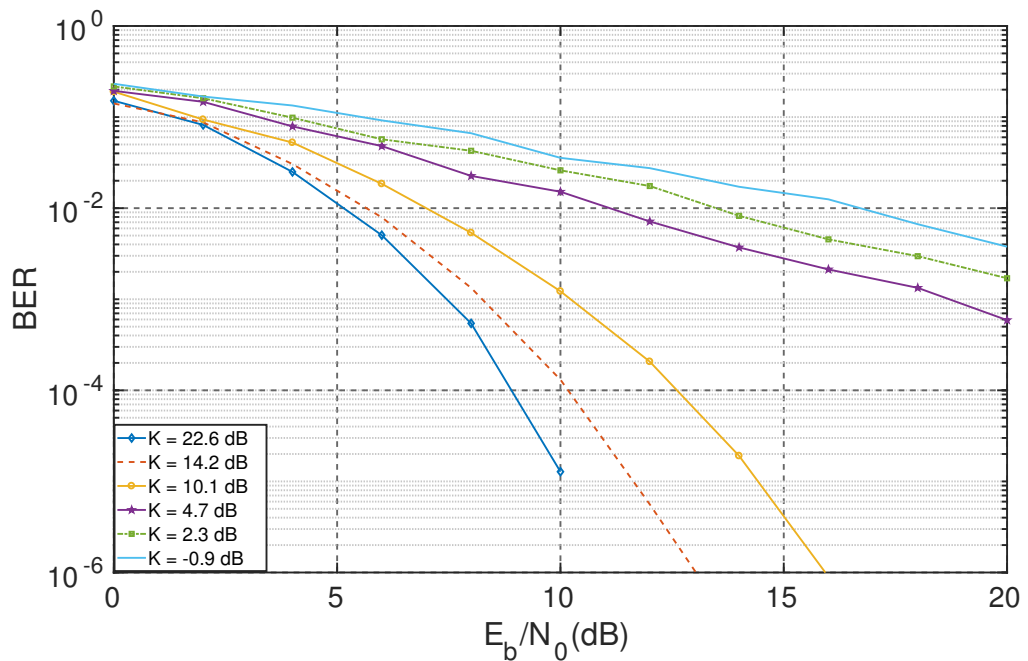


Figure 6.5: Comparison of E_b/N_0 verus BER for LTE-R OFDM-QPSK modulation with different K-factors.

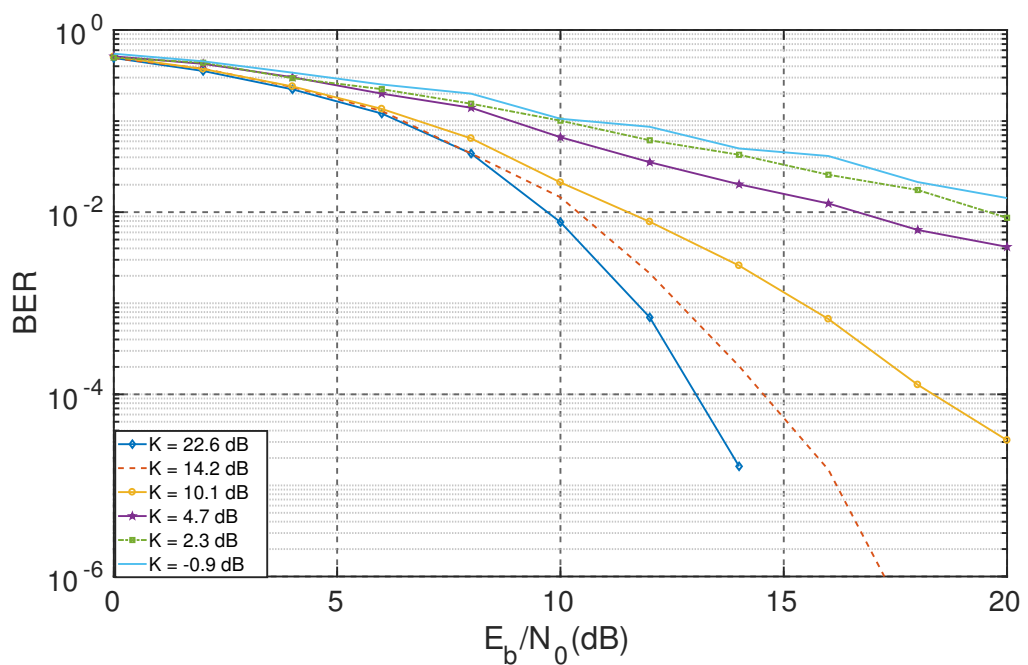


Figure 6.6: Comparison of E_b/N_0 verus BER for LTE-R OFDM-16QAM modulation with different K-factors.

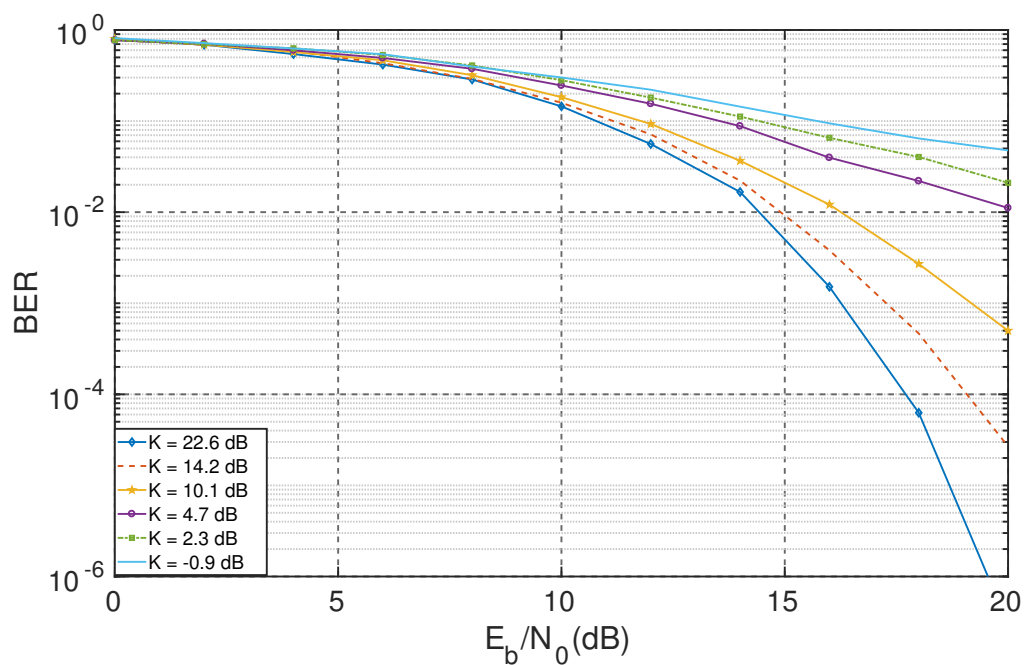


Figure 6.7: Comparison of E_b/N_0 verus BER for LTE-R OFDM-64QAM modulation with different K-factors.

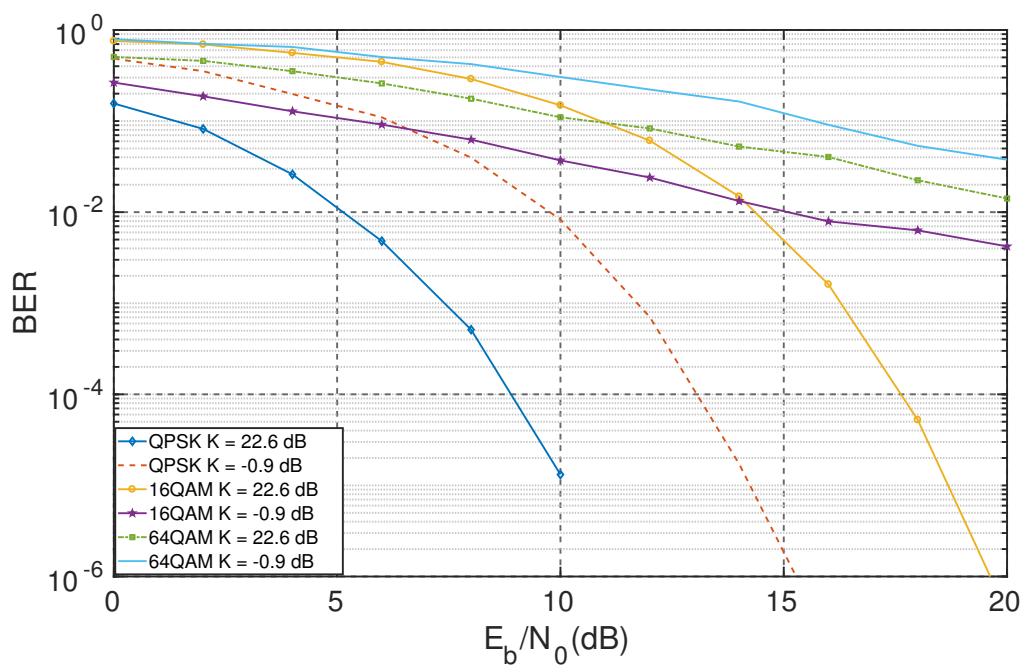


Figure 6.8: Comparison of E_b/N_0 verus BER for LTE-R OFDM modulation with different K-factors.

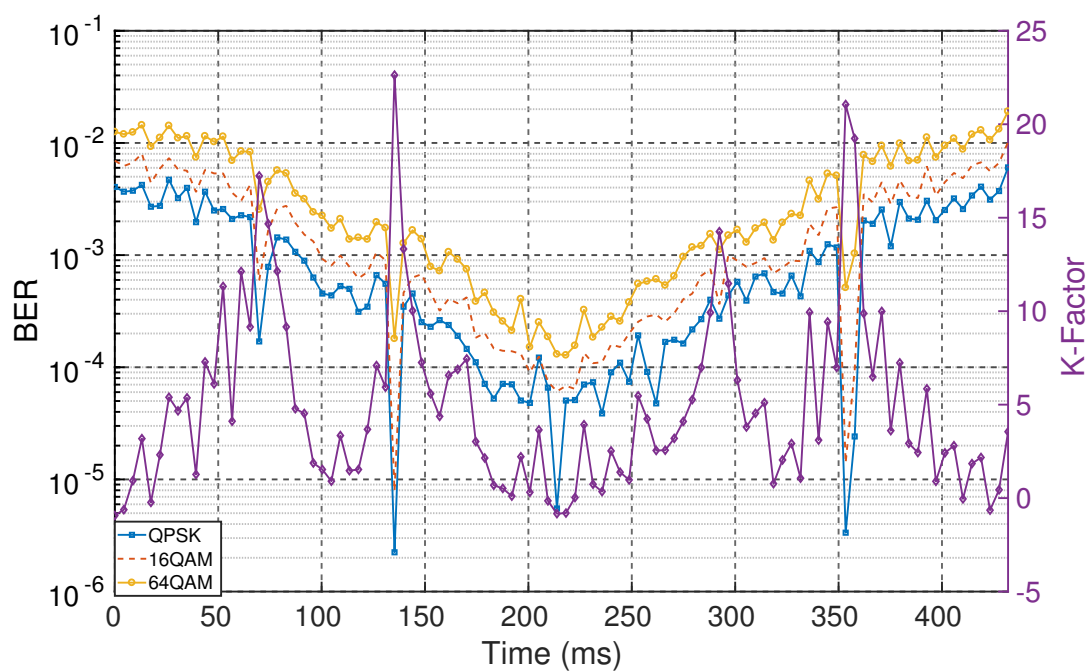


Figure 6.9: BER variation with time for HST with different modulation schemes of LTE-R. As the train moves towards the antenna the general trend of BER goes down with small-scale fluctuations due to varying K-factor.

Chapter 7

Conclusions

7.1 Research Outcomes

7.2 Future Work

Bibliography

- [1] I. F. Akyildiz, W.-Y. Lee, M. C. Vuran, and S. Mohanty, “Next generation/dynamic spectrum access/cognitive radio wireless networks: A survey,” *Computer networks*, vol. 50, no. 13, pp. 2127–2159, 2006.
- [2] Q. Zhao and B. M. Sadler, “A survey of dynamic spectrum access,” *IEEE signal processing magazine*, vol. 24, no. 3, pp. 79–89, 2007.
- [3] A. M. Wyglinski and D. Pu, *Digital communication systems engineering with software-defined radio*. Artech House, 2013.
- [4] H. Urkowitz, “Energy detection of unknown deterministic signals,” *Proceedings of the IEEE*, vol. 55, no. 4, pp. 523–531, 1967.
- [5] D. Cabric, S. M. Mishra, and R. W. Brodersen, “Implementation issues in spectrum sensing for cognitive radios,” in *Signals, systems and computers, 2004. Conference record of the thirty-eighth Asilomar conference on*, vol. 1. Ieee, 2004, pp. 772–776.
- [6] R. Tandra and A. Sahai, “Fundamental limits on detection in low snr under noise uncertainty,” in *Wireless Networks, Communications and Mobile Computing, 2005 International Conference on*, vol. 1. IEEE, 2005, pp. 464–469.
- [7] S. M. Mishra, A. Sahai, and R. W. Brodersen, “Cooperative sensing among cognitive radios,” in *Communications, 2006. ICC’06. IEEE International conference on*, vol. 4. IEEE, 2006, pp. 1658–1663.
- [8] A. Ghasemi and E. S. Sousa, “Impact of user collaboration on the performance of

- sensing-based opportunistic spectrum access,” in *Vehicular Technology Conference, 2006. VTC-2006 Fall. 2006 IEEE 64th.* IEEE, 2006, pp. 1–6.
- [9] U. G.-R. F. Group, “Gsm-r functional requirement specification (FRS),” UIC, Paris, France UIC EIRENE Technology Report, Tech. Rep. UIC Code 950, Version 7.3.0, 2012.
 - [10] G. T. 36.201, “Evolved universal terrestrial radio access (E-UTRA); lte physical layer; general description,” 3GPP, Sophia Antipolis, France, Tech. Rep. version 12.2.0, Release 12, 2015.
 - [11] K. Masur and D. Mandoc, “Lte/saethe future railway mobile radio system? long term visions on railway mobile radio technologies,” *International Union of Railways (UIC), Technical Report*, vol. 1, 2009.
 - [12] G. Tingting and S. Bin, “A high-speed railway mobile communication system based on lte,” in *Electronics and Information Engineering (ICEIE), 2010 International Conference On.* IEEE, 2010, pp. V1–414.
 - [13] K. Guan, Z. Zhong, and B. Ai, “Assessment of lte-r using high speed railway channel model,” in *Communications and Mobile Computing (CMC), 2011 Third International Conference on.* IEEE, 2011, pp. 461–464.
 - [14] H. Wei, Z. Zhong, K. Guan, and B. Ai, “Path loss models in viaduct and plain scenarios of the high-speed railway,” in *Communications and Networking in China (CHINACOM), 2010 5th International ICST Conference on.* IEEE, 2010, pp. 1–5.
 - [15] D. G. Dudley, M. Lienard, S. F. Mahmoud, and P. Degauque, “Wireless propagation in tunnels,” *IEEE Antennas and Propagation Magazine*, vol. 49, no. 2, pp. 11–26, 2007.
 - [16] J. Ma, G. Zhao, and Y. Li, “Soft combination and detection for cooperative spectrum sensing in cognitive radio networks,” *IEEE Transactions on Wireless Communications*, vol. 7, no. 11, pp. 4502–4507, 2008.

- [17] B. Shen, T. Cui, K. Kwak, C. Zhao, and Z. Zhou, "An optimal soft fusion scheme for cooperative spectrum sensing in cognitive radio network," in *Wireless Communications and Networking Conference, 2009. WCNC 2009. IEEE*. IEEE, 2009, pp. 1–5.
- [18] H. Rifà-Pous, M. J. Blasco, and C. Garrigues, "Review of robust cooperative spectrum sensing techniques for cognitive radio networks," *Wireless Personal Communications*, vol. 67, no. 2, pp. 175–198, 2012.
- [19] Y. Zeng, Y.-C. Liang, S. Zheng, and E. C. Peh, "Optimal cooperative sensing and its robustness to decoding errors," in *Communications (ICC), 2011 IEEE International Conference on*. IEEE, 2011, pp. 1–5.
- [20] J.-M. Molina-Garcia-Pardo, M. Lienard, A. Nasr, and P. Degauque, "Wideband analysis of large scale and small scale fading in tunnels," in *ITS Telecommunications, 2008. ITST 2008. 8th International Conference on*. IEEE, 2008, pp. 270–273.
- [21] T. Liu, X. Ma, R. Zhao, H. Dong, and L. Jia, "Doppler shift estimation for high-speed railway scenario," in *2016 IEEE 83rd Vehicular Technology Conference (VTC Spring)*, May 2016, pp. 1–5.
- [22] Usrp. [Online]. Available: <https://www.ettus.com/product/category/USRP-Embedded-Series/>
- [23] Rtl-sdr. [Online]. Available: <http://www rtl-sdr com/>
- [24] T. S. Rappaport *et al.*, *Wireless communications: principles and practice*. prentice hall PTR New Jersey, 1996, vol. 2.
- [25] A. Hashimoto, H. Yoshino, and H. Atarashi, "Roadmap of imt-advanced development," *IEEE Microwave Magazine*, vol. 9, no. 4, pp. 80–88, Aug 2008.
- [26] V. Chandrasekhar, J. G. Andrews, and A. Gatherer, "Femtocell networks: a survey," *IEEE Communications Magazine*, vol. 46, no. 9, pp. 59–67, September 2008.
- [27] F. Boccardi, R. Heath, A. Lozano, T. L. Marzetta, and P. Popovski, "Five disruptive technology directions for 5G," *IEEE Communications Magazine*, vol. 52, no. 2, pp. 74–80, 2014.

- [28] C.-X. Wang, F. Haider, X. Gao, X.-H. You, Y. Yang, D. Yuan, H. Aggoun, H. Haas, S. Fletcher, and E. Hepsaydir, “Cellular architecture and key technologies for 5G wireless communication networks,” *IEEE Communications Magazine*, vol. 52, no. 2, pp. 122–130, 2014. [Online]. Available: <http://ieeexplore.ieee.org/lpdocs/epic03/wrapper.htm?arnumber=6736752>
- [29] T. S. Rappaport, S. Sun, R. Mayzus, H. Zhao, Y. Azar, K. Wang, G. N. Wong, J. K. Schulz, M. Samimi, and F. Gutierrez, “Millimeter wave mobile communications for 5g cellular: It will work!” *IEEE Access*, vol. 1, pp. 335–349, 2013.
- [30] H. Elgala, R. Mesleh, H. Haas, and B. Pricope, “Ofdm visible light wireless communication based on white leds,” in *2007 IEEE 65th Vehicular Technology Conference - VTC2007-Spring*, April 2007, pp. 2185–2189.
- [31] S. Y. Seidel and H. W. Arnold, “Propagation measurements at 28 ghz to investigate the performance of local multipoint distribution service (lmds),” in *Global Telecommunications Conference, 1995. GLOBECOM '95., IEEE*, vol. 1, Nov 1995, pp. 754–757 vol.1.
- [32] M. Nekovee, “Dynamic spectrum access with cognitive radios: Future architectures and research challenges,” in *2006 1st International Conference on Cognitive Radio Oriented Wireless Networks and Communications*, June 2006, pp. 1–5.
- [33] J. Mitola, “Cognitive radio for flexible mobile multimedia communications,” in *Mobile Multimedia Communications, 1999. (MoMuC '99) 1999 IEEE International Workshop on*, 1999, pp. 3–10.
- [34] Mimo. [Online]. Available: <https://massivemimo.eu/>
- [35] A. Laya, L. Alonso, and J. Alonso-Zarate, “Is the random access channel of lte and lte-a suitable for m2m communications? a survey of alternatives.” *IEEE Communications Surveys and Tutorials*, vol. 16, no. 1, pp. 4–16, 2014.
- [36] M. Chen, J. Wan, S. González-Valenzuela, X. Liao, and V. C. Leung, “A survey of

- recent developments in home m2m networks.” *IEEE Communications Surveys and Tutorials*, vol. 16, no. 1, pp. 98–114, 2014.
- [37] F. Rusek, D. Persson, B. K. Lau, E. G. Larsson, T. L. Marzetta, O. Edfors, and F. Tufvesson, “Scaling up mimo: Opportunities and challenges with very large arrays,” *IEEE Signal Processing Magazine*, vol. 30, no. 1, pp. 40–60, 2013.
 - [38] A. M. Wyglinski, M. Nekovee, and T. Hou, *Cognitive radio communications and networks: principles and practice*. Academic Press, 2009.
 - [39] X. Hong, C.-X. Wang, M. Uysal, X. Ge, and S. Ouyang, “Capacity of hybrid cognitive radio networks with distributed vaas,” *IEEE Transactions on Vehicular Technology*, vol. 59, no. 7, pp. 3510–3523, 2010.
 - [40] W. Roh, J.-Y. Seol, J. Park, B. Lee, J. Lee, Y. Kim, J. Cho, K. Cheun, and F. Aryanfar, “Millimeter-wave beamforming as an enabling technology for 5g cellular communications: Theoretical feasibility and prototype results,” *IEEE communications magazine*, vol. 52, no. 2, pp. 106–113, 2014.
 - [41] H. T. Friis, “A note on a simple transmission formula,” *Proceedings of the IRE*, vol. 34, no. 5, pp. 254–256, 1946.
 - [42] X. Ge, H. Cheng, G. Mao, Y. Yang, and S. Tu, “Vehicular communications for 5g cooperative small-cell networks,” *IEEE Transactions on Vehicular Technology*, vol. 65, no. 10, pp. 7882–7894, 2016.
 - [43] G. Araniti, C. Campolo, M. Condoluci, A. Iera, and A. Molinaro, “Lte for vehicular networking: a survey,” *IEEE Communications Magazine*, vol. 51, no. 5, pp. 148–157, 2013.
 - [44] S. Mumtaz, K. M. S. Huq, and J. Rodriguez, “Direct mobile-to-mobile communication: Paradigm for 5g,” *IEEE Wireless Communications*, vol. 21, no. 5, pp. 14–23, 2014.
 - [45] J. Mitola and G. Q. Maguire, “Cognitive radio: making software radios more personal,” *IEEE Personal Communications*, vol. 6, no. 4, pp. 13–18, Aug 1999.

- [46] B. Barker, A. Agah, and A. M. Wyglinski, "Mission-oriented communications properties for software-defined radio configuration," *Cognitive Radio Networks*, p. 435, 2008.
- [47] S. Haykin, "Cognitive radio: brain-empowered wireless communications," *IEEE journal on selected areas in communications*, vol. 23, no. 2, 2005.
- [48] T. R. Newman, B. A. Barker, A. M. Wyglinski, A. Agah, J. B. Evans, and G. J. Minden, "Cognitive engine implementation for wireless multicarrier transceivers," *Wireless communications and mobile computing*, vol. 7, no. 9, pp. 1129–1142, 2007.
- [49] T. R. Newman, R. Rajbanshi, A. M. Wyglinski, J. B. Evans, and G. J. Minden, "Population adaptation for genetic algorithm-based cognitive radios," *Mobile networks and applications*, vol. 13, no. 5, pp. 442–451, 2008.
- [50] G. Yang, J. Wang, J. Luo, O. Y. Wen, H. Li, Q. Li, and S. Li, "Cooperative spectrum sensing in heterogeneous cognitive radio networks based on normalized energy detection," *IEEE Transactions on vehicular technology*, vol. 65, no. 3, pp. 1452–1463, 2016.
- [51] Y. Zeng and Y.-C. Liang, "Eigenvalue-based spectrum sensing algorithms for cognitive radio," *IEEE transactions on communications*, vol. 57, no. 6, 2009.
- [52] J. Mitola, "Software radios-survey, critical evaluation and future directions," in *[Proceedings] NTC-92: National Telesystems Conference*, May 1992, pp. 13/15–13/23.
- [53] R. I. Lackey and D. W. Upmal, "Speakeasy: the military software radio," *IEEE Communications Magazine*, vol. 33, no. 5, pp. 56–61, May 1995.
- [54] Xilinx-spartan-3a. [Online]. Available: <https://www.xilinx.com/products/silicon-devices/fpga/xa-spar>

Appendix A

Appendix: Heterogeneous Cooperative Spectrum Sensing Code

A.1 harddecisionpdroc.m

```
% Hard-Decision Combining Results For Sensor Nodes
clc;
close all;
clear all;

%% Parameter Initialization
N = 32;
k=4;%sensor nodes..
variance = 24.32e-9;
pfa = 0.05;
threshold = (qfuncinv(pfa)+sqrt(N)).*sqrt(N)*2*variance;
snrthreotical = -18:0.5:20;
snrlinear = 10.^ (snrthreotical/10);

%% SNR values from USRP and RTL-SDR
snrpracticalavg = [-18.23,-14.22,-13.1,-12.22,-10.35,-8.25,-5.3,-2.1,0.13,...]
```

```

1.34,2.58,3.76,8.98,11.33,12.35,13.45,15.77];
snrlinearprac = 10.^ (snrpracticalavg/10);
%% Computing Detection Probability and ROC Characteristics
pdprac = qfunc((threshold-2*N*variance.* (1+snrlinearprac))./...
    (sqrt(N.* (1+2*snrlinearprac)) * (2*variance)));
pdpracor = 1-(1-pdprac).^4;
pdpracand = pdprac.^4;
tmp1 = (1-pdprac).^2;
tmp2 = (1-pdprac);
pdpracmjr = (6*pdprac.^2).*tmp1+(4*pdprac.^3).*tmp2+pdprac.^4;

pfapracor = 1-(1-pfa).^4;
pfapracand = pfa.^4;
tmp1 = (1-pfa).^2;
tmp2 = (1-pfa);
pfapracmjr = (6*pfa.^2).*tmp1+(4*pfa.^3).*tmp2+pfa.^4;

%% ROC Characteristics...
figure(1)
hold on;
grid on;
plot(pfapracor,pdpracor(:,5), '-->', 'LineWidth', 2, 'MarkerFaceColor', 'auto');
plot(pfapracor,pdpracor(:,7), '-->', 'LineWidth', 2, 'MarkerFaceColor', 'auto');
plot(pfapracand,pdpracand(:,5), '-d', 'LineWidth', 2, 'MarkerFaceColor', 'auto');
plot(pfapracand,pdpracand(:,7), '-d', 'LineWidth', 2, 'MarkerFaceColor', 'auto');
plot(pfapracmjr,pdpracmjr(:,5), '--', 'LineWidth', 2, 'MarkerFaceColor', 'auto');
plot(pfapracmjr,pdpracmjr(:,7), '--', 'LineWidth', 2, 'MarkerFaceColor', 'auto');
xlabel('Average Probability Of False Alarm');
ylabel('Average Probability of Detection');
title('ROC Characterisitcs of Hard Decision Combining');
hold off;
set(gca, 'fontsize', 30, 'box', 'on', 'LineWidth', 2, 'GridLineStyle', '--', 'GridAlpha'
    , 0.7);
lgd = legend('OR SNR=-10.35dB', 'OR SNR=-5.3dB', 'AND SNR=-10.35dB', ...
    'AND SNR=-5.3dB', 'Majority SNR=-10.35dB', 'Majority SNR=-5.3dB');
lgd.FontSize=20;

```

```

%% Probability of detection
figure(2)
hold on;
grid on;
plot(snrpracticalavg,pdpracor,'->','LineWidth',2);
plot(snrpracticalavg,pdpracand,'-<','LineWidth',2);
plot(snrpracticalavg,pdpracmjr,'-d','LineWidth',2);
xlabel('SNR-{avg} in (dB)');
ylabel('Average Probability of Detection');
title('P_{avg} vs SNR_{avg} for Hard Decision Combining');
hold off;
set(gca,'fontsize',30,'box','on','LineWidth',2,'GridLineStyle','--','GridAlpha'
,0.7);
lgd = legend('OR Decision','AND Decision','Majority Rule Decision');
lgd.FontSize=20;
axis([-18.23 15.77 0 1])

```

A.2 softharddecisionpd.m

```

% Soft Decision Combining for sensor nodes...
%% Initializing parameters..
close all;
clear all;
N = [100,200,300,400];% Different sum factor
k=4;% Number of Sensor Nodes
variance = [24.025e-9,23.695e-9,25.678e-9,0.0323e-9];
pfa = 0.05;%Probability of false alarm
for i=1:4
threshold(i) = (qfuncinv(pfa)+sqrt(N(i)))*sqrt(N(i))*2*variance(i);
end
% SNR Values from four sensor nodes
snrpractical = [-21.45,-18.23,-15.45,-13.3,-12.67,-9.35,-2.23,-4.32,2.98,6.95,13
.57,21.78;...
-22.23,-20.22,-17.34,-15.32,-13.45,-11.27,-7.75,-5.67,2.53,4.78
,12.67,20.32;...]

```

```

-25.34,-23.34,-21.67,-20.33,-16.76,-13.38,-8.56,-6.53,0.38,1.34
,7.89,16.54;...
-27.32,-24.97,-22.34,-22.23,-17.34,-14.32,-11.35,-7.85,-2.35,-0
.98,2.38,5.98];

for i=1:4
    snrlinearprac(i,:) = 10.^ (snrpractical(i,:)/10);
end
for i=1:4
    pdprac(i,:) = qfunc((threshold(i)-2*N(i)*variance(i).* (1+snrlinearprac(i,:)))/
    ...
    (sqrt(N(i)*(1+2*snrlinearprac(i,:)))*(2*variance(i))));
end
for i=1:12
    snravg(i) = mean(snrpractical(:,i));
end
%% MNE based CS..
pdpracmne = 1-(1-pdprac(1,:)).*(1-pdprac(2,:)).*(1-pdprac(3,:)).*(1-pdprac(4,:))
;
pdpracand = mean(pdprac).^4;
pdpracm = mean(pdprac);
pdpracor = 1-(1-pdpracm).^4;
tmp1 = (1-pdpracm).^ (k-2);
tmp2 = (1-pdpracm);
pdpracmjr = (6*pdpracm.^ (k-2)).*tmp1+(4*pdpracm.^ (k-1)).*tmp2+pdpracm.^ k;
figure(1)
hold on;
grid on;
plot(snravg,pdpracmne,'-<', 'LineWidth',2, 'MarkerFaceColor','auto');
axis([-20 10 0 1])
%% EGC based CS..
snrlinearmean = 10.^ (snravg/10);
snrlinear = 10.^ (snrpractical/10);
pfa = 0.01;
M= mean(N);
threshold = mean(threshold);
for i=1:length(snravg)
    num(i) = threshold-snrlinarmean(i);

```

```

den(i) = (1/16)*((1+2*snrlinear(1,i))/N(1)+variance(1)+(1+2*snrlinear(2,i))/N(2)+variance(2)+(1+2*snrlinear(3,i))/N(3)+variance(3)+(1+2*snrlinear(4,i))/N(4)+variance(4));
pdegc(i) = qfunc(num(i)/sqrt(den(i)));
end

%% Plotting the data..
plot(snravg,pdegc,'-d','LineWidth',2,'MarkerFaceColor','auto');
plot(snravg,pdpracand,'-s','LineWidth',2,'MarkerFaceColor','auto');
plot(snravg,pdpracor,'-s','LineWidth',2,'MarkerFaceColor','auto');
plot(snravg,pdpracmjr,'->','LineWidth',2,'MarkerFaceColor','auto');
title('P_{avg} vs SNR_{avg} for Soft and Hard Decision Combining');
xlabel('SNR_{avg} in (dB)');
ylabel('Average Probability of Detection');
set(gca,'fontsize',30,'box','on','LineWidth',2,'GridLineStyle','--','GridAlpha',0.7);
legend('MNE Combining','EGC Combining','AND Rule','OR Rule','Majority Rule');

```

A.3 spectrumsenseusrp.py

```

#!/usr/bin/env python
#
# Copyright 2005,2007,2011 Free Software Foundation, Inc.
#
# This file is part of GNU Radio
#
# GNU Radio is free software; you can redistribute it and/or modify
# it under the terms of the GNU General Public License as published by
# the Free Software Foundation; either version 3, or (at your option)
# any later version.
#
# GNU Radio is distributed in the hope that it will be useful,
# but WITHOUT ANY WARRANTY; without even the implied warranty of
# MERCHANTABILITY or FITNESS FOR A PARTICULAR PURPOSE. See the
# GNU General Public License for more details.

```

```
#  
# You should have received a copy of the GNU General Public License  
# along with GNU Radio; see the file COPYING. If not, write to  
# the Free Software Foundation, Inc., 51 Franklin Street,  
# Boston, MA 02110-1301, USA.  
  
#  
  
from gnuradio import gr, eng_notation  
from gnuradio import blocks  
from gnuradio import audio  
from gnuradio import filter  
from gnuradio import fft  
from gnuradio import uhd  
from gnuradio.eng_option import eng_option  
from optparse import OptionParser  
import sys  
import math  
import struct  
import threading  
from datetime import datetime  
import time  
from gnuradio.wxgui import stdgui2, fftsink2, form  
import wx  
  
sys.stderr.write("Warning: this may have issues on some machines+Python version  
combinations to seg fault due to the callback in bin_statistics.\n\n")  
  
class ThreadClass(threading.Thread):  
    def run(self):  
        return  
  
class tune(gr.feval_dd):  
    """  
    This class allows C++ code to callback into python.  
    """  
    def __init__(self, tb):  
        gr.feval_dd.__init__(self)
```

```

        self.tb = tb

    def eval(self, ignore):
        """
        This method is called from blocks.bin_statistics_f when it wants
        to change the center frequency. This method tunes the front
        end to the new center frequency, and returns the new frequency
        as its result.
        """

    try:
        new_freq = self.tb.set_next_freq()
        while(self.tb.msgq.full_p()):
            time.sleep(0.1)
        return new_freq

    except Exception, e:
        print "tune: Exception: ", e


class parse_msg(object):
    def __init__(self, msg):
        self.center_freq = msg.arg1()
        self.vlen = int(msg.arg2())
        assert(msg.length() == self.vlen * gr.sizeof_float)
        t = msg.to_string()
        self.raw_data = t
        self.data = struct.unpack('%df' % (self.vlen,), t)

class my_top_block(gr.top_block):
    def __init__(self):
        gr.top_block.__init__(self)

        usage = "usage: %prog [options] min_freq max_freq"
        parser = OptionParser(option_class=eng_option, usage=usage)

```

```

parser.add_option("-a", "--args", type="string", default="",
                  help="UHD device device address args [default=%default
                        ]")
parser.add_option("", "--spec", type="string", default=None,
                  help="Subdevice of UHD device where appropriate")
parser.add_option("-A", "--antenna", type="string", default=None,
                  help="select Rx Antenna where appropriate")
parser.add_option("-s", "--samp-rate", type="eng_float", default=1e6,
                  help="set sample rate [default=%default]")
parser.add_option("-g", "--gain", type="eng_float", default=None,
                  help="set gain in dB (default is midpoint)")
parser.add_option("", "--tune-delay", type="eng_float",
                  default=0.25, metavar="SECS",
                  help="time to delay (in seconds) after changing
                        frequency [default=%default]")
parser.add_option("", "--dwell-delay", type="eng_float",
                  default=0.25, metavar="SECS",
                  help="time to dwell (in seconds) at a given frequency
                        [default=%default]")
parser.add_option("-b", "--channel-bandwidth", type="eng_float",
                  default=6.25e3, metavar="Hz",
                  help="channel bandwidth of fft bins in Hz [default=%
                        default]")
parser.add_option("-l", "--lo-offset", type="eng_float",
                  default=0, metavar="Hz",
                  help="lo_offset in Hz [default=%default]")
parser.add_option("-q", "--squelch-threshold", type="eng_float",
                  default=None, metavar="dB",
                  help="squelch threshold in dB [default=%default]")
parser.add_option("-F", "--fft-size", type="int", default=None,
                  help="specify number of FFT bins [default=samp_rate/
                        channel_bw]")
parser.add_option("", "--real-time", action="store_true", default=False,
                  help="Attempt to enable real-time scheduling")

(options, args) = parser.parse_args()
if len(args) != 2:

```

```

parser.print_help()
sys.exit(1)

self.channel_bandwidth = options.channel_bandwidth

self.min_freq = eng_notation.str_to_num(args[0])
self.max_freq = eng_notation.str_to_num(args[1])

if self.min_freq > self.max_freq:
    # swap them
    self.min_freq, self.max_freq = self.max_freq, self.min_freq

if not options.realtime:
    realtime = False
else:
    # Attempt to enable realtime scheduling
    r = gr.enable_realtime_scheduling()
    if r == gr.RT_OK:
        realtime = True
    else:
        realtime = False
    print "Note: failed to enable realtime scheduling"

# build graph
self.u = uhd.usrp_source(device_addr=options.args,
                         stream_args=uhd.stream_args('fc32'))

# Set the subdevice spec
if(options.spec):
    self.u.set_subdev_spec(options.spec, 0)

# Set the antenna
if(options.antenna):
    self.u.set_antenna(options.antenna, 0)

self.u.set_samp_rate(options.samp_rate)
self.usrp_rate = usrp_rate = self.u.get_samp_rate()

```

```

    self.lo_offset = options.lo_offset

    if options.fft_size is None:
        self.fft_size = int(self.usrp_rate/self.channel_bandwidth)
    else:
        self.fft_size = options.fft_size

    self.squelch_threshold = options.squelch_threshold

    s2v = blocks.stream_to_vector(gr.sizeof_gr_complex, self.fft_size)

    mywindow = filter.window.blackmanharris(self.fft_size)
    ffter = fft.fft_vcc(self.fft_size, True, mywindow, True)
    power = 0
    for tap in mywindow:
        power += tap*tap
    c2mag = blocks.complex_to_mag_squared(self.fft_size)
    self.freq_step = self.nearest_freq((0.75 * self.usrp_rate),
                                       self.channel_bandwidth)
    self.min_center_freq = self.min_freq + (self.freq_step/2)
    nsteps = math.ceil((self.max_freq - self.min_freq) / self.freq_step)
    self.max_center_freq = self.min_center_freq + (nsteps * self.freq_step)
    self.next_freq = self.min_center_freq
    tune_delay = max(0, int(round(options.tune_delay * usrp_rate /
                                   self.fft_size))) # in fft_frames
    dwell_delay = max(1, int(round(options.dwell_delay * usrp_rate /
                                   self.fft_size))) # in fft_frames
    self.msgq = gr.msg_queue(1)
    self._tune_callback = tune(self) # hang on to this to keep it
                                    from being GC'd
    stats = blocks.bin_statistics_f(self.fft_size, self.msgq,
                                    self._tune_callback, tune_delay,
                                    dwell_delay)
    self.connect(self.u, s2v, ffter, c2mag, stats)

    if options.gain is None:

```

```

g = self.u.get_gain_range()
options.gain = float(g.start() + g.stop()) / 2.0

self.set_gain(options.gain)
print "gain =", options.gain

def set_next_freq(self):
    target_freq = self.next_freq
    self.next_freq = self.next_freq + self.freq_step
    if self.next_freq >= self.max_center_freq:
        self.next_freq = self.min_center_freq

    if not self.set_freq(target_freq):
        print "Failed to set frequency to", target_freq
        sys.exit(1)

    return target_freq


def set_freq(self, target_freq):
    """
    Set the center frequency we're interested in.

    Args:
        target_freq: frequency in Hz
        @rypte: bool
    """

    r = self.u.set_center_freq(uhd.tune_request(target_freq, rf_freq=
        target_freq + self.lo_offset), rf_freq_policy=
        uhd.tune_request.POLICY_MANUAL))

    if r:
        return True

    return False

```

```

def set_gain(self, gain):
    self.u.set_gain(gain)

def nearest_freq(self, freq, channel_bandwidth):
    freq = round(freq / channel_bandwidth, 0) * channel_bandwidth
    return freq

def main_loop(tb):

    def bin_freq(i_bin, center_freq):
        freq = center_freq - (tb.usrp_rate / 2) + (tb.channel_bandwidth * i_bin)
        return freq

    bin_start = int(tb.fft_size * ((1 - 0.25) / 2))
    bin_stop = int(tb.fft_size - bin_start)
    fid = open("./usrp.dat", "wb")
    while 1:
        m = parse_msg(tb.msgq.delete_head())
        for i_bin in range(bin_start, bin_stop):
            center_freq = m.center_freq
            freq = bin_freq(i_bin, center_freq)
            power_db = 10 * math.log10(m.data[i_bin] / tb.usrp_rate)
            signal = m.data[i_bin] / (tb.usrp_rate)

            if (power_db > tb.squelch_threshold) and (freq >= tb.min_freq) and (
                freq <= tb.max_freq):
                print freq, signal, power_db
                fid.write(struct.pack('<f', signal))
    fid.close()#closing the file

if __name__ == '__main__':
    t = ThreadClass()
    t.start()

    tb = my_top_block()
    try:
        tb.start()

```

```

    main_loop(tb)

except KeyboardInterrupt:
    pass

```

A.4 gnuradiortlsdrsense.py

```

#!/usr/bin/env python2
# -*- coding: utf-8 -*-

#####
# GNU Radio Python Flow Graph
# Title: DTV Spectrum Sensing
# Author: Gill
# Description: Frequency Sweep for UHF White Spaces
# Generated: Fri Mar 10 14:30:20 2017
#####

if __name__ == '__main__':
    import ctypes
    import sys
    if sys.platform.startswith('linux'):
        try:
            x11 = ctypes.cdll.LoadLibrary('libX11.so')
            x11.XInitThreads()
        except:
            print "Warning: failed to XInitThreads()"

from PyQt4 import Qt
from gnuradio import blocks
from gnuradio import eng_notation
from gnuradio import fft
from gnuradio import gr
from gnuradio import qtgui
from gnuradio.eng_option import eng_option
from gnuradio.fft import window

```

```
from gnuradio.filter import firdes
from optparse import OptionParser
import numpy as np
import osmosdr
import sip
import sys
import time

class spectrum_sensing(gr.top_block, Qt.QWidget):

    def __init__(self):
        gr.top_block.__init__(self, "DTv Spectrum Sensing")
        Qt.QWidget.__init__(self)
        self.setWindowTitle("DTv Spectrum Sensing")
        try:
            self.setWindowIcon(Qt.QIcon.fromTheme('gnuradio-grc'))
        except:
            pass
        self.top_scroll_layout = Qt.QVBoxLayout()
        self.setLayout(self.top_scroll_layout)
        self.top_scroll = Qt.QScrollArea()
        self.top_scroll.setStyle(Qt.QFrame.NoFrame)
        self.top_scroll_layout.addWidget(self.top_scroll)
        self.top_scroll.setWidgetResizable(True)
        self.top_widget = Qt.QWidget()
        self.top_scroll.setWidget(self.top_widget)
        self.top_layout = Qt.QVBoxLayout(self.top_widget)
        self.top_grid_layout = Qt.QGridLayout()
        self.top_layout.addLayout(self.top_grid_layout)

        self.settings = Qt.QSettings("GNU Radio", "spectrum_sensing")
        self.restoreGeometry(self.settings.value("geometry").toByteArray())

#####
# Variables
#####
```

```

    self.samp_rate = samp_rate = int(2e6)
    self.freq = freq = 450e6
    self.N = N = 1000

#####
# Blocks
#####
self.rtlsdr_source_0 = osmosdr.source( args="numchan=" + str(1) + " " +
    ' ')
self.rtlsdr_source_0.set_time_source('external', 0)
self.rtlsdr_source_0.set_sample_rate(samp_rate)
self.rtlsdr_source_0.set_center_freq(freq, 0)
self.rtlsdr_source_0.set_freq_corr(0, 0)
self.rtlsdr_source_0.set_dc_offset_mode(2, 0)
self.rtlsdr_source_0.set_iq_balance_mode(0, 0)
self.rtlsdr_source_0.set_gain_mode(True, 0)
self.rtlsdr_source_0.set_gain(15, 0)
self.rtlsdr_source_0.set_if_gain(15, 0)
self.rtlsdr_source_0.set_bb_gain(15, 0)
self.rtlsdr_source_0.set_antenna('', 0)
self.rtlsdr_source_0.set_bandwidth(0, 0)

self.qtgui_freq_sink_x_0 = qtgui.freq_sink_c(
    1024, #size
    firdes.WIN_BLACKMAN_hARRIS, #wintype
    0, #fc
    samp_rate, #bw
    "Recieved Signal", #name
    1 #number of inputs
)
self.qtgui_freq_sink_x_0.set_update_time(0.10)
self.qtgui_freq_sink_x_0.set_y_axis(-120, 0)
self.qtgui_freq_sink_x_0.set_y_label('Relative Gain', 'dB')
self.qtgui_freq_sink_x_0.set_trigger_mode(qtgui.TRIG_MODE_FREE, 0.0, 0,
    "")
self.qtgui_freq_sink_x_0.enable_autoscale(True)
self.qtgui_freq_sink_x_0.enable_grid(True)

```

```

    self.qtgui_freq_sink_x_0.set_fft_average(1.0)
    self.qtgui_freq_sink_x_0.enable_axis_labels(True)
    self.qtgui_freq_sink_x_0.enable_control_panel(False)

    if not True:
        self.qtgui_freq_sink_x_0.disable_legend()

    if "complex" == "float" or "complex" == "msg-float":
        self.qtgui_freq_sink_x_0.set_plot_pos_half(not True)

    labels = ['', '', '', '', '',
              '', '', '', '', '']
    widths = [2, 1, 1, 1, 1,
              1, 1, 1, 1, 1]
    colors = ["blue", "red", "green", "black", "cyan",
              "magenta", "yellow", "dark red", "dark green", "dark blue"]
    alphas = [1.0, 1.0, 1.0, 1.0, 1.0,
              1.0, 1.0, 1.0, 1.0, 1.0]
    for i in xrange(1):
        if len(labels[i]) == 0:
            self.qtgui_freq_sink_x_0.set_line_label(i, "Data {0}".format(i))
        else:
            self.qtgui_freq_sink_x_0.set_line_label(i, labels[i])
        self.qtgui_freq_sink_x_0.set_line_width(i, widths[i])
        self.qtgui_freq_sink_x_0.set_line_color(i, colors[i])
        self.qtgui_freq_sink_x_0.set_line_alpha(i, alphas[i])

    self._qtgui_freq_sink_x_0_win = sip.wrapinstance(
        self.qtgui_freq_sink_x_0.pyqwidget(), Qt.QWidget)
    self.top_layout.addWidget(self._qtgui_freq_sink_x_0_win)
    self.fft_vxx_0 = fft.fft_vcc(1024, True, (window.blackmanharris(1024)),
                                True, 1)
    self.blocks_vector_to_stream_0 = blocks.vector_to_stream(gr.sizeof_float
                                                          *1, 1024)
    self.blocks_stream_to_vector_0 = blocks.stream_to_vector(
        gr.sizeof_gr_complex*1, 1024)
    self.blocks_moving_average_xx_0 = blocks.moving_average_ff(N, 1, 4000)

```

```

self.blocks_file_sink_2_0 = blocks.file_sink(gr.sizeof_float*1, '/home/
gill/Desktop/ms-thesis/gr-spectrumsensing/grc/rtl-sdr_sensing/
Results/snr_check.dat', False)
self.blocks_file_sink_2_0.set_unbuffered(False)
self.blocks_complex_to_mag_squared_0 = blocks.complex_to_mag_squared
(1024)

#####
# Connections
#####
self.connect((self.blocks_complex_to_mag_squared_0, 0), (
    self.blocks_vector_to_stream_0, 0))
self.connect((self.blocks_moving_average_xx_0, 0), (
    self.blocks_file_sink_2_0, 0))
self.connect((self.blocks_stream_to_vector_0, 0), (self.fft_vxx_0, 0))
self.connect((self.blocks_vector_to_stream_0, 0), (
    self.blocks_moving_average_xx_0, 0))
self.connect((self.fft_vxx_0, 0), (self.blocks_complex_to_mag_squared_0,
    0))
self.connect((self.rtlsdr_source_0, 0), (self.blocks_stream_to_vector_0,
    0))
self.connect((self.rtlsdr_source_0, 0), (self.qtgui_freq_sink_x_0, 0))

def closeEvent(self, event):
    self.settings = Qt.QSettings("GNU Radio", "spectrum_sensing")
    self.settings.setValue("geometry", self.saveGeometry())
    event.accept()

def get_samp_rate(self):
    return self.samp_rate

def set_samp_rate(self, samp_rate):
    self.samp_rate = samp_rate
    self.rtlsdr_source_0.set_sample_rate(self.samp_rate)
    self.qtgui_freq_sink_x_0.set_frequency_range(0, self.samp_rate)

def get_freq(self):

```

```
    return self.freq

def set_freq(self, freq):
    self.freq = freq
    self.rtlsdr_source_0.set_center_freq(self.freq, 0)

def get_N(self):
    return self.N

def set_N(self, N):
    self.N = N
    self.blocks_moving_average_xx_0.set_length_and_scale(self.N, 1)

def main(top_block_cls=spectrum_sensing, options=None):

    from distutils.version import StrictVersion
    if StrictVersion(Qt.qVersion()) >= StrictVersion("4.5.0"):
        style = gr.prefs().get_string('qtgui', 'style', 'raster')
        Qt.QApplication.setGraphicsSystem(style)
    qapp = Qt.QApplication(sys.argv)

    tb = top_block_cls()
    tb.start()
    tb.show()

    def quitting():
        tb.stop()
        tb.wait()
    qapp.connect(qapp, Qt.SIGNAL("aboutToQuit()"), quitting)
    qapp.exec_()

if __name__ == '__main__':
    main()
```

Appendix B

Appendix: LTE-R Analysis Code

B.1 kfactordist.m

```
% Calculating K-factor for the tunnel environment for HST
clear all;
close all;
clc;

%% Creating a doppler profile for high speed raiway scenario..
Ds = 30;%Initial Distance between tx and rx times 2..
Dmin = 2;% Distance between raiway tracks and leaky feeder cables...
Kf = [];
fc = 3e9;%center frequency..
c = 3e8;
v = 138.9;%300;
t = linspace(0, (2*Ds)/v(1),100);
fd = (v*fc)/3e8;%maximum doppler frequency...
costheta = zeros(size(t));%angle between BS and MS
d1 = [];
for i=1:length(t)
    d1(i) = sqrt(2^2+(Ds/2-v(1)*t(i))^2);%distance between tx and rx..
    if t(i) >=0 && t(i)<= (Ds/v)
        costheta(i) = ((Ds/2)-v*t(i))./sqrt(Dmin^2+(Ds/2-v*t(i))^2);
    end
end
```

```

elseif t(i) > (Ds/v) && t(i)<=(2*Ds)/v
costheta(i) = (-1.5*Ds+v*t(i))./sqrt(Dmin^2+(-1.5*Ds+v*t(i))^2);
end
end
fs = fd*costheta;
thetadeg = acosd(costheta);
fc_wds = fc-fs;
lambda = c./fc_wds;
Cin = 5-((0.1*1.8e10)./fc_wds)*1j;
C = Cin;
gammanum = C.*sind(thetadeg)-sqrt(Cin-(cosd(thetadeg)).^2);
gammaden = C.*sind(thetadeg)+sqrt(Cin-(cosd(thetadeg)).^2);
gamma = gammanum./gammaden;
ht = 6.1;%height of feeder cable
hr = 4.2;%height of the train
var1 = sqrt(d1.^2+(ht+hr)^2);
var2 = sqrt(d1.^2+(ht-hr)^2);
phase = (((2*pi)./lambda).* (var1-var2))*180/pi;
gammad = atan2d(imag(gamma),real(gamma));
phasegamma = abs(cosd(gammad-phase));
K = abs(gamma).^2+2*abs(gamma).*phasegamma;
Kf = 10*log10(1./K);

```

B.2 bercalculation.m

```

% Demonstration of Eb/N0 Vs SER for M-QAM modulation scheme
clc;
load Kf;
load t;
%-----Input Fields-----
%% QPSk
bitsperframe=1e3; %Number of input symbols
EbN0dB = [linspace(0,20,50) fliplr(linspace(0,20,50))]; %Define EbN0dB range for
simulation
M=4; %for QPSk modulation.

```

```

hMod = comm.RectangularQAMModulator('ModulationOrder',M);
const = step(hMod, (0:3)');

%-----
refArray = 1/sqrt(2)*const';
k=log2(M);

totPower=15; %Total power of LOS path & scattered paths

EsN0dB = EbN0dB + 10*log10(k);
biterrsim = zeros(size(EsN0dB));
%---Generating a uniformly distributed random numbers in the set [0,1,2,...,M-1]
data=ceil(M.*rand(bitsperframe,1))-1;
s=refArray(data+1); %QPSK Constellation mapping with Gray coding
%--- Reference Constellation for demodulation and Error rate computation--
refI = real(refArray);
refQ = imag(refArray);
%---Place holder for Symbol Error values for each Es/N0 for particular M value--
index=1;
u=1;
% Kf = 4.9;
K = 10.^ (Kf/10);
for x=EsN0dB
    sn=sqrt(K(u)/(K(u)+1)*totPower); %Non-Centrality Parameter
    sigma=totPower/sqrt(2*(K(u)+1));
    h=((sigma*randn(1,bitsperframe)+sn)+li*(randn(1,bitsperframe)*sigma+0));
    numerr = 0;
    numBits = 0;
    while numerr < 100 && numBits < 1e7
        %-----
        %Channel Noise for various Es/N0
        %-----
        %Adding noise with variance according to the required Es/N0
        noiseVariance = 1/(10.^ (x/10));%Standard deviation for AWGN Noise
        noiseSigma = sqrt(noiseVariance/2);
        %Creating a complex noise for adding with M-QAM modulated signal
        %Noise is complex since M-QAM is in complex representation
        noise = noiseSigma*(randn(size(s))+li*randn(size(s)));
        received = s.*h + noise;

```

```

%-----I-Q Branching-----
received = received./h;
r_i = real(received);
r_q = imag(received);
%---Decision Maker-Compute  $(r_i - s_i)^2 + (r_q - s_q)^2$  and choose the
smallest
r_i_repmat = repmat(r_i,M,1);
r_q_repmat = repmat(r_q,M,1);
distance = zeros(M,bitsperframe); %place holder for distance metric
minDistIndex=zeros(bitsperframe,1);
for j=1:bitsperframe
    %---Distance computation -  $(r_i - s_i)^2 + (r_q - s_q)^2$  -----
    distance(:,j) = (r_i_repmat(:,j)-refI').^2+(r_q_repmat(:,j)-refQ').
        ^2;
    %---capture the index in the array where the minimum distance occurs
    [dummy,minDistIndex(j)]=min(distance(:,j));
end
y = minDistIndex - 1;
%-----Symbol Error Rate Calculation
-----
dataCap = y;
numerr = sum(dataCap~=data)+numerr;
numBits = numBits+bitsperframe;
disp(numerr);
end
symErrSimulatedqpsk(1,index) = numerr/numBits;
biterrsime(1,index) = symErrSimulatedqpsk(1,index)/k;
index=index+1;
% u=u+1;
end

%% 16 QAM
bitsperframe=1e3; %Number of input symbols
EbN0dB = [linspace(0,10,50) fliplr(linspace(0,10,50))]; %Define EbN0dB range for
simulation
M=16; %for QPSK modulation.
hMod = comm.RectangularQAMModulator('ModulationOrder',M);

```

```

const = step(hMod, (0:M-1)');
%-----
refArray =1/sqrt(10)*const';
k=log2(M);
totPower=10; %Total power of LOS path & scattered paths

EsN0dB = EBN0dB + 10*log10(k);
biterrsim = zeros(size(EsN0dB));
%---Generating a uniformly distributed random numbers in the set [0,1,2,...,M-1]
data=ceil(M.*rand(bitsperframe,1))-1;
s=refArray(data+1); %QPSK Constellation mapping with Gray coding
%--- Reference Constellation for demodulation and Error rate computation--
refI = real(refArray);
refQ = imag(refArray);
%---Place holder for Symbol Error values for each Es/N0 for particular M value--
index=1;
u=1;
K = 10.^ (Kf/10);
for x=EsN0dB
    numerr = 0;
    numBits = 0;
    while numerr < 100 && numBits < 1e7
        sn=sqrt(K(u) / (K(u)+1)*totPower); %Non-Centrality Parameter
        sigma=totPower/sqrt(2*(K(u)+1));
        h=((sigma*randn(1,bitsperframe)+sn)+li*(randn(1,bitsperframe)*sigma+0));
        %-----
        %Channel Noise for various Es/N0
        %-----
        %Adding noise with variance according to the required Es/N0
        noiseVariance = 1/(10.^ (x/10));%Standard deviation for AWGN Noise
        noiseSigma = sqrt(noiseVariance/2);
        %Creating a complex noise for adding with M-QAM modulated signal
        %Noise is complex since M-QAM is in complex representation
        noise = noiseSigma*(randn(size(s))+li*randn(size(s)));
        received = s.*h + noise;
        %-----I-Q Branching-----

```

```

received = received./h;
r_i = real(received);
r_q = imag(received);
%---Decision Maker-Compute  $(r_i - s_i)^2 + (r_q - s_q)^2$  and choose the
smallest
r_i_repmat = repmat(r_i,M,1);
r_q_repmat = repmat(r_q,M,1);
distance = zeros(M,bitsperframe); %place holder for distance metric
minDistIndex=zeros(bitsperframe,1);
for j=1:bitsperframe
%---Distance computation -  $(r_i - s_i)^2 + (r_q - s_q)^2$  -----
distance(:,j) = (r_i_repmat(:,j)-refI').^2+(r_q_repmat(:,j)-refQ').
^2;
%---capture the index in the array where the minimum distance occurs
[dummy,minDistIndex(j)]=min(distance(:,j));
end
y = minDistIndex - 1;
%-----Symbol Error Rate Calculation
-----
dataCap = y;
numerr = sum(dataCap~=data)+numerr;
numBits = numBits+bitsperframe;
disp(numerr);
end
symErrSimulatedqam(l,index) = numerr/numBits;
biterrsime(l,index) = symErrSimulatedqam(l,index)/k;
index=index+1;
u=u+1;
end

%% 64 QAM Modulation...
bitsperframe=1e3; %Number of input symbols
EbN0dB = [linspace(0,10,50) fliplr(linspace(0,10,50))]; %Define EbN0dB range for
simulation
M=64; %for QPSK modulation.
hMod = comm.RectangularQAMModulator('ModulationOrder',M);
const = step(hMod, (0:M-1)');

```

```
%-----
refArray =1/sqrt(42)*const';
k=log2(M);
totPower=10; %Total power of LOS path & scattered paths
EsN0dB = EbN0dB + 10*log10(k);
biterrsime = zeros(size(EsN0dB));
%---Generating a uniformly distributed random numbers in the set [0,1,2,...,M-1]
data=ceil(M.*rand(bitsperframe,1))-1;
s=refArray(data+1); %QPSK Constellation mapping with Gray coding
%--- Reference Constellation for demodulation and Error rate computation--
refI = real(refArray);
refQ = imag(refArray);
%---Place holder for Symbol Error values for each Es/N0 for particular M value--
index=1;
u=1;
K = 10.^ (Kf/10);
for x=EsN0dB
    sn=sqrt(K(u) / (K(u)+1)*totPower); %Non-Centrality Parameter
    sigma=totPower/sqrt(2*(K(u)+1));
    h=((sigma*randn(1,bitsperframe)+sn)+1i*(randn(1,bitsperframe)*sigma+0));
    numerr = 0;
    numBits = 0;
    while numerr < 100 && numBits < 1e7
        %-----
        %Channel Noise for various Es/N0
        %-----
        %Adding noise with variance according to the required Es/N0
        noiseVariance = 1/(10.^(x/10));%Standard deviation for AWGN Noise
        noiseSigma = sqrt(noiseVariance/2);
        %Creating a complex noise for adding with M-QAM modulated signal
        %Noise is complex since M-QAM is in complex representation
        noise = noiseSigma*(randn(size(s))+1i*randn(size(s)));
        received = s.*h + noise;
        %-----I-Q Branching-----
        received = received./h;
        r_i = real(received);
        r_q = imag(received);
```

```

%---Decision Maker-Compute  $(r_i-s_i)^2+(r_q-s_q)^2$  and choose the
smallest
r_i_repmat = repmat(r_i,M,1);
r_q_repmat = repmat(r_q,M,1);
distance = zeros(M,bitsperframe); %place holder for distance metric
minDistIndex=zeros(bitsperframe,1);
for j=1:bitsperframe
    %---Distance computation -  $(r_i-s_i)^2+(r_q-s_q)^2$  -----
    distance(:,j) = (r_i_repmat(:,j)-refI').^2+(r_q_repmat(:,j)-refQ').
        ^2;
    %---capture the index in the array where the minimum distance occurs
    [dummy,minDistIndex(j)]=min(distance(:,j));
end
y = minDistIndex - 1;
%-----Symbol Error Rate Calculation
-----
dataCap = y;
numerr = sum(dataCap~=data)+numerr;
numBits = numBits+bitsperframe;
disp(numerr);
end
symErrSimulatedqam64(1,index) = numerr/numBits;
biterrsime(1,index) = symErrSimulatedqam64(1,index)/k;
index=index+1;
u=u+1;
end

%%
fig = figure;
semilogy(t*1e3,symErrSimulatedqpsk(1,:),'-d','LineWidth',2);
hold on;
grid on;
semilogy(t*1e3,symErrSimulatedqam(1,:),'-d','LineWidth',2);
semilogy(t*1e3,symErrSimulatedqam64(1,:),'-d','LineWidth',2);
xlabel('Time (ms)');
ylabel('Bit Error Rate (Pb)');
title(['BER For OFDM Under Rician Fading Environment Inside Tunnel']);

```

```
set(gca,'fontsize',30,'box','on','LineWidth',2,'GridLineStyle','--','GridAlpha'  
,0.7);  
axis([0 max(t)*1e3 10e-7 0])  
lgd = legend('QPSK','16QAM','64QAM');  
lgd.FontSize=20;
```